Aerospace Science and Technology 119 (2021) 107090

Contents lists available at ScienceDirect

Aerospace Science and Technology

www.elsevier.com/locate/aescte

An experimental study on the detrimental effects of deicing fluids on the performance of icephobic coatings for aircraft icing mitigation

Zichen Zhang [a], Lusi A [b], Haiyang Hu [a], Xianglan Bai [b], Hui Hu [a,*]

[a] Department of Aerospace Engineering, Iowa State University, Ames, IA, 50011, USA
[b] Department of Mechanical Engineering, Iowa State University, Ames, IA, 50011, USA

ARTICLE INFO

Article history:
Received 2 June 2021
Received in revised form 29 August 2021
Accepted 30 August 2021
Available online 9 September 2021
Communicated by Muguru Chandrasekhara

Keywords:
Aircraft anti-/de-icing
Deicing fluids
Icephobic coatings
Inflight icing mitigation

ABSTRACT

An experimental investigation was conducted to examine the detrimental effects induced by deicing fluids used for aircraft ground deicing on the performance of icephobic coatings for aircraft inflight icing mitigation. Commonly used superhydrophobic surface (SHS) and polytetrafluoroethylene (PTFE or Teflon®) were selected as the representative icephobic coatings in the present study. Test plates and airfoil/wing models coated with SHS and PTFE coatings were immersed into two kinds of deicing fluids (i.e., Type-I and Type-IV deicing fluids) to simulate the scenario of spraying deicing fluids onto aircraft surfaces for ground deicing at airports. Then, the deicing fluids were drained off from the icephobic coated surfaces to imitate their shedding off from airframe surfaces after aircraft takeoff. Variations of the surface wettability and ice adhesion characteristics on the icephobic coated surfaces were examined before and after immersion into the deicing fluids. Advanced diagnostic systems, including scanning electron microscopy (SEM), Fourier transformed infrared spectroscopy (FTIR) and energy dispersive X-ray spectroscopy (EDS), were used to reveal the changes in the surface topology and chemistry characteristics to elucidate the underlying physical and chemical "contaminations" induced by the deicing fluids to the icephobic coatings. An icing tunnel testing campaign was also conducted to demonstrate the detrimental effects induced by the contaminations of the deicing fluids on the dynamic ice accretion processes on icephobic coated airfoil/wing models. It was revealed that spraying Type-1 deicing fluid for ground deicing would have only very minor (i.e., to the SHS) or no effect (i.e., to the PTFE) on the performance of the icephobic coatings. However, spraying Type-IV deicing fluid onto airframe surfaces would degrade the performance of the icephobic coatings significantly and totally deteriorate the effectiveness of the icephobic coatings for aircraft inflight icing mitigation.

1. Introduction

Aircraft icing has been widely recognized as a severe weather hazard to flight safety in cold climates [1–3]. Aircraft operating in cold weathers must be equipped with anti-/de-icing mechanisms; otherwise, mission delays and even mission cancellations/abortions may occur. The most frequently observed aircraft icing events are the ice-buildup over airframe surfaces when airplanes are exposed to frozen precipitation at airports. Aircraft icing may also occur during the flight when small, super-cooled, airborne water droplets, which make up clouds and fog, freeze upon impacting onto airframe surfaces, which is called aircraft inflight icing. Ice accumulation over airframe surface has been found to degrade the aerodynamic performance of an airplane significantly by increasing drag while decreasing lift. The importance of proper ice control for aircraft operation in cold climates was highlighted by many aircraft crashes like the Continental Connection Flight 3407 crashed in Buffalo, New York on February 14, 2009 due to ice buildup on its wings killing all 49 people aboard and 1 person on the ground as the airplane hit a residential home [4]. While deicing fluids are commonly used to remove/prevent ice accretion over airframe surfaces for ground de-icing operation at airports prior to takeoff [5], various anti-/de-icing systems have also been developed for aircraft inflight icing mitigation to ensure safe and efficient aircraft operation under atmospheric icing conditions [6–8].

As described in Parent and Ilinca [9], all anti-/de-icing systems can generally be classified into two categories: active and passive methods. While active methods rely on energy input from an external system for anti-/de-icing operation, passive methods take advantage of physical properties of airframe surfaces (e.g., surface wettability) to prevent/delay ice formation/accretion. Current active anti-/de-icing strategies used for aircraft inflight icing

* Corresponding author.
E-mail address: huhui@iastate.edu (H. Hu).

https://doi.org/10.1016/j.ast.2021.107090
1270-9638/

mitigation suffer from various drawbacks, including being too complex, too heavy or draw too much power to be effective [7,10,11]. For example, while pneumatic de-icing systems with rubber boots have been used to break off ice chunks accreted at airfoil leading edges during the flight, they are usually quite heavy and sometime unreliable [12]. Ultrasonic and mechanical de-icing solutions are not easily integrated into existing aircraft and pose foreign object damage (FOD) hazards to aero-engines [12]. While electric heating [13], plasma heating [14], and hot air injection [15] systems have been used to melt out accreted ice by heating airframe surfaces, they are usually very inefficient and have highly demanding power requirements. They can also cause damage to composite-based substrate materials due to overheating. Furthermore, the melt water may simply run back and re-freeze at downstream locations to cause uncontrolled runback ice accretion [12]. Due to the obvious advantages of light weight, zero energy input and low installation cost, passive anti-/de-icing approaches of utilizing hydro-/ice-phobic coatings are attracting increasing attentions in recent years for use as viable strategies for aircraft inflight icing mitigation [2,16,17].

Inspired by the outstanding self-cleaning capability of lotus leaf and duck feathers [18–20], a number of studies have been conducted in recent years to develop coatings to make superhydrophobic surfaces (i.e., SHS), on which water droplets bead up and drip off rapidly when the surface is slightly inclined [21]. It is well known that all SHS possess textured/rough surfaces [22,23]. When a macroscopic water droplet comes in contact with a textured SHS coated surface, it adopts the so-called *Cassie-Baxter state* [24] with air trapped inside the surface textures beneath the droplet. Since the macroscopic water droplet is supported on thousands of air pockets, it beads up and displays very high contact angles (i.e., typically $> 150^\circ$ for SHS). One attractive application of SHS, in addition to the extraordinary water-repellency, is their potentials to reduce/delay accumulation of snow and ice on solid surfaces. SHS coatings were found to delay/suppress ice accumulation at low temperatures down to $-30\,^\circ$C [21,25]. It was also reported that SHS coatings can be icephobic with the ice adhesion strength on SHS coated surfaces being only about 10% of the case without the SHS coatings [26]. The recent study of Waldman and Hu [27] demonstrated that, due to the superhydrophobic nature and smaller ice adhesion strength over a SHS coated wing surface, aerodynamic shear forces exerted by the incoming airflow would be more readily sweep away impinged water mass and accreted ice structures from the SHS coated airfoil/wing model. As a result, a much less ice coverage was observed over the SHS coated airfoil surface, in comparison to the airfoil surface without the SHS coating. Liu et al. [28] carried out an explorative study to leverage a SHS coating to effectively suppress the ice accretion on the rotating propellers of unmanned-aerial-systems (UAS) under different icing conditions. Gao et al. [29] demonstrated a novel hybrid anti-/de-icing system by integrating a SHS coating with minimized surface heating at the airfoil leading edge to effectively prevent ice accretion over the entire airfoil surface at a much lower power cost than conventional brutally-heating methods (i.e., saving up to 90% of the required power consumption for anti-/de-icing operation). More recently, Zhang et al. [30] conducted an experimental campaign to evaluate the mechanical durability of a SHS coating to resist "rain erosion" damages, i.e., the ability to prevent the coating materials wearing away from the substrates caused by the continuous impingement of water droplets at high impacting speeds up to 100 m/s.

In addition to SHS coatings, Polytetrafluoroethylene (i.e., PTFE in short), which is a synthetic fluoropolymer of tetrafluoroethylene and also commonly known as Teflon®, has also been suggested for various anti-/de-icing applications in recent years [2,31–33]. As reported in Menini & Farzaneh [32], since PTEF has a low surface energy and a strong hydrogen type of bonding with water molecules, it appears to be one of the best hydrophobic and icephobic substances. In addition to being an outstanding non-stick coating, PTFE has also been found to be an excellent lubricant to reduce friction, wear, erosion, and corrosion because of the supper strong carbon–fluorine bonds. As reported by Cao et al. [34], after applying PTFE to coat a titanium alloy surface, droplets were found to be more readily bouncing off and rolling away from the PTFE coated surface, even at low temperatures (i.e., minimizing ice accretion eventually). Freezing process of droplets on PTFE coated surface was also found to become much longer than that on the uncoated y surface (i.e., delaying ice formation effectively). Furthermore, since PTFE has much higher wear resistance and can resist freezing and thawing almost permanently, which is highly desirable to resist the "rain erosion" damages pertinent to aircraft inflight icing [2,30]. Yu et al. [35] fabricated a thin PTFE coating on an aluminum substrate by using an electrostatic self-assembly method, and reported that a large ice layer accreted over the PTFE coated surface would be much more readily to fall off, demonstrating the great potentials of using PTFE coatings for effective anti-/de-icing over large-scale aircraft wing surfaces.

Since deicing fluids (i.e., aqueous solutions of propylene and ethylene glycol along with other chemical additives) can effectively suppress the freezing point of water and melt ice even at the temperature as low as $-20\,^\circ$C [36], they are routinely used to melt and remove the buildup of ice structures over airframe surfaces for ground de-icing operation at airports prior to takeoff [5]. There are four kinds of standard aircraft deicing fluids: Type I, II, III and IV [37]. While Type-I fluid is the thinnest among all the deicing fluids, spraying hot Type-I deicing fluid is widely used to effectively remove accreted ice on airframe surfaces for ground de-icing [38]. Type II, III and IV fluids are thickened by adding thickening agents to elongate the duration of protection (i.e., up to 4 hours) [38]. Type II, III and IV deicing fluids are designed to be non-Newtonian shear-thinning fluids so that they can run off from the wing surfaces quickly during the takeoff [39]. In the present study, Type-I and Type-IV deicing fluids are selected since they are the most widely used deicing fluids for aircraft ground de-icing operation at the airports [40].

While spraying deicing fluids over airframe surfaces to melt/remove the buildup of ice structures is widely used as a standard procedure for ground anti-/de-icing operation [37], utilizing hydro-/ice-phobic coatings to cover airframe surfaces are demonstrated to be a promising strategy for aircraft inflight icing mitigation. However, the potential interferences/interactions between the deicing fluids and icephobic coatings are not fully explored. For example, while the hydrophobicity and icephobicity of a surface are directly related to its surface topology and chemistry characteristics [2,32], some chemical compounds included in deicing fluids (e.g., thickening agents, propylene glycol and surfactants) may potentially affect the performances of hydro-/ice-phobic coatings by influencing the surface topology and chemistry characteristics of the surface coatings (i.e., changing the properties of the surface coatings physically or/and chemically) [38]. While a number of previous studies were conducted to examine the changes in the runback dynamics of wind-driven deicing fluids over hydrophilic [37,41] and icephobic surfaces [42], very little can be found in the literature to examine the effects of the deicing fluids on the anti-icing performance of icephobic coatings for aircraft icing mitigation.

In the present study, a comprehensive experimental campaign was conducted to evaluate the detrimental effects of the deicing fluids commonly used for aircraft ground de-icing operations on the anti-icing performance of the icephobic coatings for aircraft inflight icing mitigation. Commonly used superhydrophobic surface (SHS) and polytetrafluoroethylene (PTFE or Teflon®) were selected as the representative icephobic coatings in the present

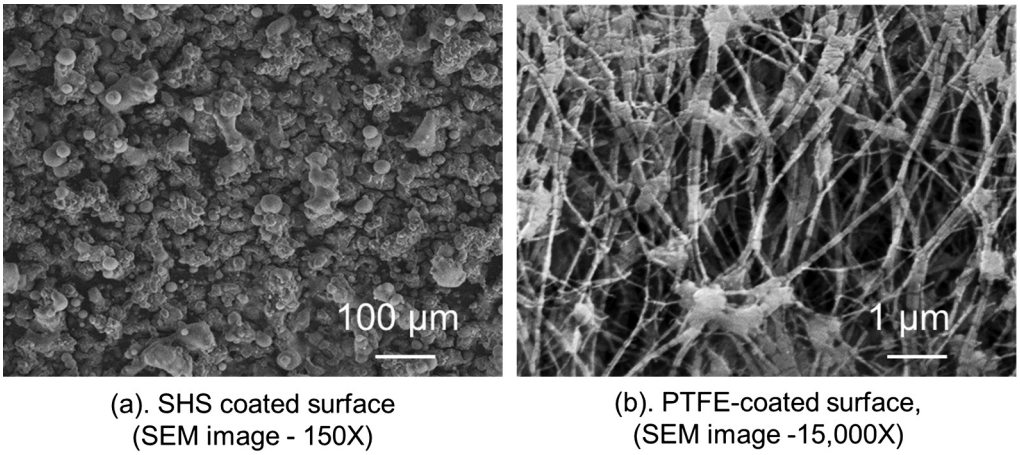

Fig. 1. Acquired SEM images to reveal the topologies of the SHS and PTFE coated surfaces.

study. A set of test plates and airfoil/wing models coated with the icephobic coatings were first immersed into two different kinds of deicing fluids (i.e., Type-I and Type-IV deicing fluids) to simulate the scenario of spraying deicing fluids onto airframe surfaces for the ground de-icing operation at the airports. After immersion for pre-selected time durations (i.e., up to 60 minutes), the test models were taken out from the deicing fluids and placed over an inclined bench for 48 hours to drain off the deicing fluids from the test models to imitate the scenario of the deicing fluids shedding off from the airframe surfaces after takeoff from the airport. The surface wettability and ice adhesion strength on the test plates were characterized before and after immersion into the deicing fluids. Advanced diagnostic systems, including scanning electron microscopy (SEM), Fourier transformed infrared spectroscopy (FTIR) and energy dispersive X-ray spectroscopy (EDS), were used to examine the changes in the surface topology and chemistry characteristics of the icephobic coated surfaces in order to elucidate the underlying physical and chemical "contaminations" induced by the deicing fluids. By leveraging the icing research tunnel available at Iowa State University (i.e., ISU-IRT), an icing experiment campaign was also conducted to demonstrate the detrimental effects induced by deicing fluids on the dynamic ice accretion process over the surfaces of the airfoil/wing models coated with icephobic coatings.

2. Experimental setup and test models

2.1. Icephobic coatings and deicing fluids used in the present study

In the present study, two kinds of icephobic coatings/surfaces, i.e., a SHS coating and a PTFE-based surface, were selected due to their promising potentials (i.e., being hydrophobic and having very low ice adhesion strength) for aircraft icing mitigation [28,43]. A set of square-shaped aluminum test plates (i.e., made of aluminum 6061 alloy substrate with 50 mm in width and 6.5 mm in thickness) were prepared for the present study. The test plates were carefully polished by using sandpapers grits ranging from 220 to 2000 to enhance the surface homogeneity. SHS coated surfaces were made by spraying a commercially available SHS coating – Hydrobead® onto the test plates. As shown from the SEM image given in Fig. 1(a), micro-/nano-scaled, hierarchical surface roughness/textures were found to be generated over the surface of the test plate after applying the SHS coating, resulting in the superhydrophobicity [44]. The same SHS coating has been widely used in recent studies for aircraft icing mitigation [16,27,28,45]. PTFE-based icephobic surfaces were made by laminating porous PTFE membranes purchased from Sterlitech® to cover the top surfaces of the test plates. The porous PTFE membranes have glutinous

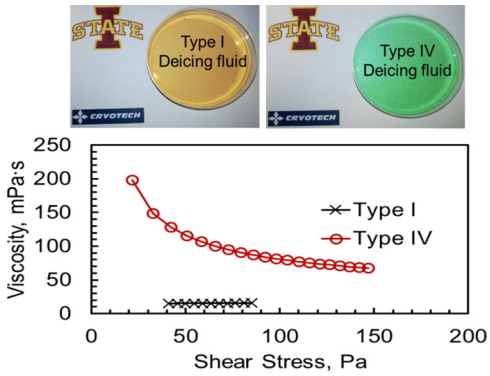

Fig. 2. Measured viscosity of the deicing fluids at a temperature of 20 °C. (For interpretation of the colors in the figure(s), the reader is referred to the web version of this article.)

polypropylene backers which can stick firmly onto the test plates. As revealed clearly from the SEM image given in Fig. 1(b), the PTFE coated surface are nanofibrous with an average pore size of less than 200 nm. In addition to the SHS and PTFE coatings, an Enamel coating (i.e., Rust-Oleum Stops Rust®) was also used as the reference baseline in the present study. It should be noted that, Enamel coating is a very commonly used protective/decorative coating for metal, glass, or ceramic ware, which has been widely used as the reference coating in previous aircraft anti-/de-icing studies [28,46].

Type-I and Type-IV deicing fluids used for the present study were provided by Cryotech Deicing Technology Company. Type-I deicing fluid was diluted with 45% water in volume, as suggested by the manufacturer to improve its deicing performance. According to the material safety data sheet (MSDS), both of Type-I and Type-IV deicing fluids contain 50% propylene glycol, 49% water and less than 1% proprietary properties. The viscosity of the diluted Type-I deicing fluid and Type-IV deicing fluid were measured by using a rheometer (Black Perl, Cannon Instrument) at a temperature of 20 °C, and the measurement results are given in Fig. 2. It can be seen clearly that, while the diluted Type-I deicing fluid was found to be a Newtonian fluid with a low viscosity of ~ 15 mPa · s, Type-IV deicing fluid is a non-Newtonian viscous liquid with a varying viscosity at different shear stress levels. Type-I and Type-IV deicing fluids are in green and orange colors, respectively.

During the experiment, the SHS and PTEF coated test plates were immersed into the deicing fluids for pre-selected time durations (i.e., ranging from 1.0 minute to 60.0 minutes) to simulate the scenario of the deicing fluids being sprayed onto aircraft surfaces for the ground de-icing operation and remained on the airframe surfaces with different waiting times before takeoff. To imitate the

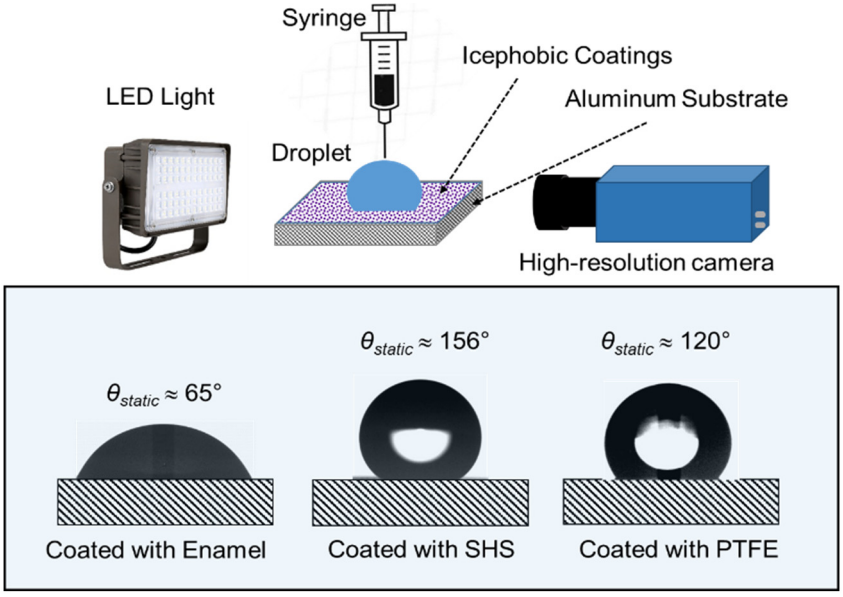

Fig. 3. Experimental setup used to quantify the droplet contact angles on the test plates.

Table 1
Measured droplet contact angles and ice adhesion strengths on different surfaces.

Tested surface	Wettability	Static contact angle, θ_{static}	Ice adhesion strength, τ_{ice}
Uncoated surface	Hydrophilic	$60° \pm 5°$	450 kPa ± 20 KPa
Enamel	Hydrophilic	$65° \pm 5°$	14.00 kPa ± 50 Kpa
PTFE	Hydrophobic	$120° \pm 5°$	20 kPa ± 5 Kpa
SHS	Superhydrophobic	$156° \pm 5°$	105 kPa ± 10 Kpa

shedding off of the deicing fluids from airframe surfaces after aircraft takeoff, the test plates were placed onto a tilted bench for 48 hours to drain out all the deicing fluids from the surfaces of test plates. The test plates were also put in a heated vacuum oven (Across International) at a constant temperature of 60 °C for 24 hours in order to evaporate/dry out any liquid remaining on the SHS and PTFE coated test plates.

2.2. Characterization of the wettability and ice adhesion strength on the test surfaces

Fig. 3 shows the experimental setup used in the present study to quantify the surface wettability of the SHS and PTFE coated test plates (i.e., in term of the contact angles of water droplets, θ_{static}) before and after being immersed into the deicing fluids. With the similar procedure as that described in Korhonen et al. [47], water droplets with a specific volume (i.e., 10 μL for the present study) were placed over the surfaces of the SHS and PTFE coated test plates to determine the droplets contact angles. The images of the water droplets were recorded by using high-resolution digital camera (PCO^{TM}-1200, PCO Tech. Inc.) with a Nikon Micro lens. The recorded images were analyzed by using MATLAB-based image processing software developed "in-house" to determine the droplet contact angles on the test plates [28]. The contact angle measurements were repeated at least 10 times for each test cases in order to reduce the measurement uncertainty.

The measured contact angles of water droplets on the test plates coated with different surface coatings before immersion into deicing fluids are summarized in Table 1. It can be seen clearly that, before applying any surface coatings, the contact angle of water droplets on the uncoated aluminum surface was found to be smaller than 90° (i.e., $\theta_{static} = 60°$), confirming the hydrophilic nature of uncoated aluminum surfaces. In comparison, after applying different icephobic coatings over the test plates, while the

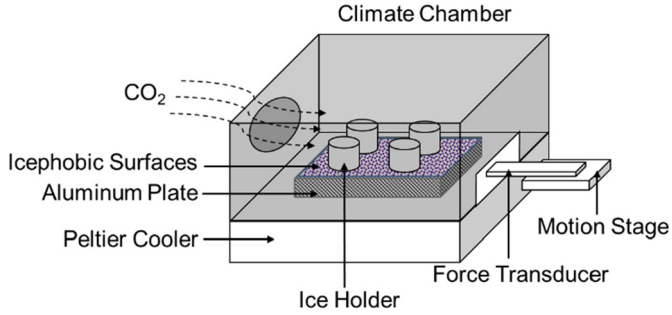

Fig. 4. Experimental setup used for the ice adhesion strength measurements.

droplet contact angle over the PTFE coated surface was found to increase to about 120° (i.e., $\theta_{static} = 120°$, which is hydrophobic), the corresponding angle on the SHS coated surface becomes 156° (i.e., $\theta_{static} > 150°$, which is superhydrophobic). The static contact angle over the Enamel coated surface was found to be about 65° ($\theta_{static} = 65°$), which agrees with the measured value reported by Liu et al. [28].

Ice adhesion strength, τ_{ice}, is an important measure to characterize the icephobicity of a surface [48]. A lower ice adhesion strength over a solid surface indicates that the accreted ice structures would be much more likely be removed by applying external forces, such as the shear forces exerted by the incoming airflow around the airframe surface, which is highly desirable for aircraft inflight icing mitigation. In the present study, an ice adhesion measurement system similar as that described in Meuler et al. [49] was used to quantify the ice adhesion strength on the test plates coated with different coatings. As shown schematically in Fig. 4, the test rig consists of a temperature-controlled climate chamber to house a digitally controlled Peltier cooler (TETech CP061 and TC-48-20) and a linear actuator with integrated motion con-

troller (Newport CONEX-LTA-HS) to drive a force-torque transducer (JR3-30E12A4) mounted to an aluminum force probe. The force signals were recorded by using a 16-bit data acquisition card (NI PCI-6052E) connected to a host computer. 3D-printed cylindrical-shaped ice molds (i.e., 8.0 mm in diameter) filled with 0.5 mL deionized water in each molds were used to generate ice samples on the test plate [50]. With the test plate being firmly attached to the Peltier cooler, the surface temperature of the test plate was well controlled at pre-selected frozen-cold temperatures for the ice adhesion strength measurements. After the test plate was maintained at the pre-selected frozen-cold temperature (e.g., at $-10\,^{\circ}C$ for all the test cases of the present study) for over 1.0 hour, the force probe was driven to push the ice molds with a translation velocity of 0.5 mm/s until the ice samples were sheared off completely from the test plate [49]. The ice adhesion strength was then taken as the maximum force-per-area observed as ice samples were sheared off [51]. The ice adhesion measurements were repeated 10 times for each test cases to determine the mean and standard deviation values of the measurement results.

The measured ice adhesion strengths on the different test surfaces before immersion into deicing fluids are also given in Table 1. It can be seen quantitatively that, the ice adhesion strength over the uncoated aluminum surface was found to be around 450 kPa, which is within the range of the result reported in Saleema et al. [52] for bare aluminum surfaces. After applying Enamel coating to cover the aluminum substrate, the ice adhesion strength was found to increase to 1,400 kPa, which agrees with the measured value reported by Yu et al. [28]. In comparison, the ice adhesion strengths were found to be only 105 kPa and 20 kPa on the SHS and PTFE coated surfaces, respectively. It confirms that the SHS and PTFE coated surfaces are icephobic, which agree with the findings of previous studies to suggest that they are very promising for aircraft icing mitigation.

2.3. Characterization of surface topology and chemistry of the test surfaces

In order elucidate the underlying physics for a better understanding about the effects of the deicing fluids on the icephobic coatings, a set of advanced surface diagnostic systems were used in the present study to characterize the surface topology and chemistry characteristics of the icephobic coated test surfaces before and after immersion into the deicing fluids. Fourier-transform infrared spectroscopy (FTIR) [53] is a technique widely used to measure functional groups and organic mass over a solid surface for various applications. In the present study, a FTIR system (Thermo Scientific Nicolet iS10) was used to identify the changes of the functional groups on the test surfaces before and after immersion into the deicing fluids. The wavenumber of the FTIR analysis ranged from 500 cm^{-1} to 4000 cm^{-1} and each sample was scanned 32 times at a resolution of 0.5 cm^{-1}. FTIR analyses were repeated 5 times on each sample in order to reduce the measurement uncertainty.

A field-emission scanning electron microscopy (SEM) (FEI Quanta 250) was used to in the present study characterize the surface topology characteristics of the SHS and PTFE coated test plates before and after immersion into the deicing fluids. The Everhart-Thorley secondary electron detector (ETD) and annular backscattered electron detector (ABS) were used for acquiring surface topology images. Prior to the SEM measurements, the test surfaces were coated with a 3 nm layer of Iridium by a sputtering coating machine to make them conductive. In the present study, accelerating voltage of the SEM was set to be 10 kV to achieve high-resolution measurements. A low vacuum mode (30 Pa) was used to acquire high-quality images of the surface topology on SHS coated surfaces in order to avoid the sample charging problem. A high vacuum mode was used to acquire the surface topologies of the PTFE and Enamel coated surfaces. An energy-dispersive X-ray spectroscopy (EDS, Oxford low-Z spectrometer) with a large area (80 mm^2) silicone drift detector (SDD) was also used to detect the emitted X-ray signals from the tested surfaces and characterize the surface elemental composition. Further information about using FTIR and the SEM-EDS analysis for surface characterization can be found at Alus et al. [54] and Jing et al. [55].

2.4. Airfoil/wing models and icing research tunnel used for the ice accretion experiments

Six sets of identical airfoil/wing models, which have NACA0012 profile in the cross-section shape and chord length of 150 mm, were made to conduct ice accretion experiments in an icing research tunnel to demonstrate the detrimental effects of the deicing fluids on the anti-icing performance of icephobic coatings for aircraft icing mitigation. By using the same procedure described above, the airfoil/wing models coated with the different coatings (i.e., SHS, PTEF and Enamel coatings) were immersed into either Type-I or Type-IV deicing fluids for 60 minutes. After the deicing fluids were drained off completely from the airfoil surfaces, the airfoil/wing models were mounted into an icing research tunnel for ice accretion experiments.

The ice accretion experiments were performed by leveraging the unique Icing Research Tunnel available at Iowa State University (i.e., ISU-IRT). As shown schematically in Fig. 5, ISU-IRT is a multifunctional icing research tunnel with a test section of 2.0 m in length $\times$ 0.4 m in width $\times$ 0.4 m in height and optically transparent side walls. ISU-IRT was equipped with a 30-hp fan/motor unit (Baldor™) to drive airflow circling inside ISU-IRT with a maximum wind speed up to 60 m/s in the test section. The tunnel is refrigerated via a heat exchanger, which is chilled by a 40-hp compressor (Vilter™), to cool the airflow inside ISU-IRT down to $-25\,^{\circ}C$. An array of 8 spray nozzle/atomizers (IKEUCHI BIMV-11002) were mounted at the entrance of the contraction section of ISU-IRT to inject micro-sized water droplets (i.e., averaged size of 20 μm) in the airflows [56]. By manipulating the water flow rate supplied to the spray nozzles/atomizers, liquid water content (LWC) in airflow inside ISU-IRT can be adjusted from 0.1 g/m^3 to 5.0 g/m^3. In summary, ISU-IRT can be used to simulate various atmospheric icing phenomena over a wide range of icing conditions (i.e., from dry rime to extremely wet glaze ice conditions). By using ISU-IRT, extensive studies have been carried out in recent years to investigate icing physics and develop anti-/de-icing strategies for various engineering applications [57–61].

As shown schematically in Fig. 5, the airfoil/wing model was installed in the middle the test section of ISU-IRT with the incoming airflow approaching the test model horizontally. The angle of attack of the airfoil/wing models was set to be zero (i.e., AOA = 0.0 deg.) in relation to the incoming airflow. While a high-power LED light unit (RPS Studio Light, Model RS-5620) was used to provide low-flicker illumination during the icing experiments, a high-speed imaging system (PCO – Dimax™ camera with 2000 pixel by 2000 pixel and frame rate of up to 10,000 frames per second) was used to record the dynamic ice accretion processes over the surfaces of the airfoil/wing models before and after immersion into deicing fluids.

3. Measurement results and discussions

3.1. Variations of the surface wettability and ice adhesion strengths on test surfaces coated with different icephobic coatings before and after immersion into deicing fluids

In the present study, the variations of the surface wettability (i.e., in the term of the droplet contact angle) and ice adhesion

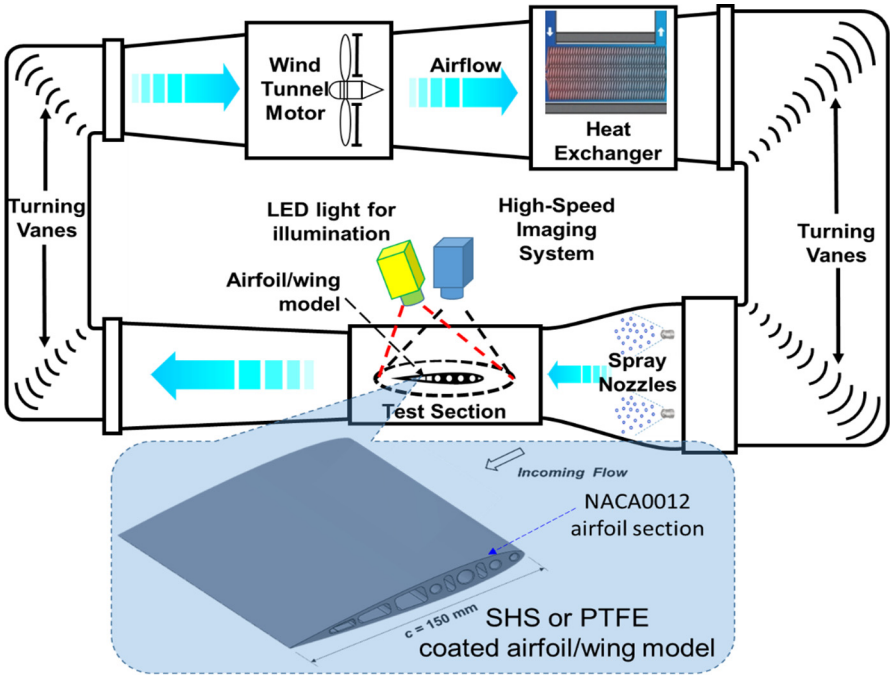

Fig. 5. Schematics of ISU-IRT and the airfoil/wing models used for icing accretion experiments.

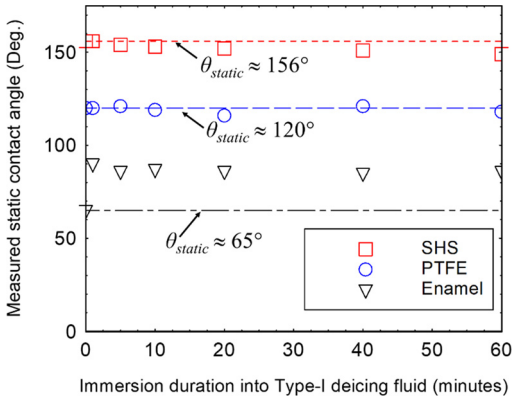

Fig. 6. Measured static contact angles on the surfaces coated with various coatings before and after immersion into Type-I deicing fluid.

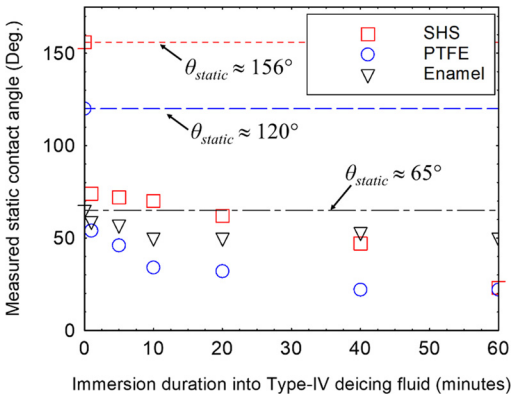

Fig. 7. Measured static contact angle on the surfaces coated with various coatings before and after immersion into Type-IV deicing fluid.

strengths on the test surfaces coated with icephobic coatings (i.e., the SHS and PTFE coatings) were characterized in order to evaluate the effects of the deicing fluids on the icephobic coatings. Fig. 6 and Fig. 7 give the measured droplets contact angles (i.e., θ_{static}) on the test plates coated with surface coatings before and after immersion into Type-I and Type-IV deicing fluids with different immersion durations.

As shown quantitatively for the measurement data given in Fig. 6, the droplet contact angles on the SHS coated surfaces were found to decrease slightly after immersion into Type-I deicing fluid. The measured values were found to decrease very slowly as the immersion time increases. After immersion into Type-I deicing fluids for about 60 minutes, the droplet contact angle on the SHS coated surface was found to decrease to about $\theta_{static} \approx 148°$, which is slightly smaller than the original value of $\theta_{static} \approx 156°$ before the immersion. The droplet contact angles on the PTFE coated surface were found be almost unchanged with the scattering range of the measured values within the measurement uncertainty margin of $\pm 5°$. It indicates that, even after being immersed into Type-I deicing fluid for 60 minutes, while the PTFE coated surface would be able to keep its hydrophobicity nature almost unchanged, the SHS coated surfaces were still found to be almost superhydrophobic. In summary, it was found that the wettability of the icephobic coatings (i.e., both SHS and PTFE coatings) would be almost unaffected by Type-I deicing fluid.

Interestingly, the droplet contact angle on Enamel coated surface was found to increase substantially after immersion into Type-I deicing fluid. More specifically, the droplet contact angle on Enamel coated surface was found to increase from $\theta_{static} \approx 65°$ to nearly $\theta_{static} \approx 90°$ after immersion into Type-I deicing fluid for 60 minutes. It indicates that the hydrophilic Enamel surface was found to become almost hydrophobic after immersion into Type-I deicing fluid.

The effects of Type-IV deicing fluid on the wettability of the icephobic coated surfaces were found to become much more complicated. As described above, even though the test plates were mounted on an inclined bench for 48 hours to drain off Type-IV deicing fluid completely from the test surfaces, and then put into a heated vacuum chamber for 24 hours to evaporate/dry out all the remaining liquid on the test surfaces, the measured droplet contact angles on both the SHS and PTFE coated surfaces were found to be decrease dramatically after being immersed into Type-IV deicing fluid. As revealed quantitatively from the measurement data given in Fig. 7, even though the test plates were immersed into

Table 2
Measured ice adhesion strength on the test surfaces before and after immersion into different deicing fluids (Unit: kPa).

Different tested surface	Surfaces before immersion into deicing fluids	Surfaces after immersion into Type-I fluid with different immersion duration (min.)					
		1	5	10	20	40	60
PTFE	20	22	20	20	18	22	21
SHS	120	290	310	340	360	370	390
Enamel	1,400	1280	1180	1090	1080	1040	1030
Different tested surface	Surfaces before immersion into deicing fluids	Surfaces after immersion into Type-IV fluid with different immersion duration (min.)					
		1	5	10	20	40	60
PTFE	20	250	270	350	380	560	640
SHS	120	320	410	530	600	610	620
Enamel	1,400	1500	1530	1470	1500	1490	1540

Type-IV fluid for only 1.0 minute, the droplet contact angle on the SHS coated surface was found to be reduced dramatically from its original value of $\theta_{static} \approx 156^\circ$ (i.e., being superhydrophobic) to only $\theta_{static} \approx 64^\circ$ (i.e., becoming hydrophilic), the corresponding values on the PTEF coated surface changed from $\theta_{static} \approx 120^\circ$ (i.e., being hydrophobic) to $\theta_{static} \approx 54^\circ$ (i.e., becoming hydrophilic). The wettability degradation of the SHS and PTFE coated surfaces was found to become worse and worse as the immersion time increases. The SHS and PTFE coated surfaces were found to becoming highly hydrophilic with the droplet contact angles on both SHS and PTFE becoming only about $\theta_{static} \approx 23^\circ$ after immersion into Type-IV deicing fluid for 60 minutes. It indicates that the SHS and PTFE coatings would lose their hydrophobicity and became hydrophilic for good, once they are "contaminated" by Type-IV deicing fluid. Draining out Type-IV deicing fluid from the SHS and PTFE coated surfaces for 48 hours and then drying the "contaminated" surfaces for another 24 hours to further evaporate all the liquids remaining on the test surface would not be able to recover their original hydrophobicity. It should be noted that, since the wettability of a surface is directly related to the physical properties (e.g., surface topology) and chemistry characteristics of the surface [44], the measurement results given above suggested that some changes/damages must have been made to the SHS and PTFE coated surfaces (i.e., the surface characteristics were changed either physically or/and chemically) due to the "contamination" of Type-IV deicing fluid. Further discussions/analysis about the effects of Type-IV deicing fluid on the SHS and PTFE coated surface will be given later based on the SEM images, FTIR and EDS analysis results to be presented in the following sections.

It can also be seen that, even though it was not as dramatic as those on the SHS and PTFE coated surfaces, the wettability of Enamel coated surface also degraded substantially after immersion into Type-IV deicing fluid. As shown clearly in Fig. 7, the droplet contact angle on the Enamel coated surface was found to decrease from $\theta_{static} \approx 65^\circ$ to about $\theta_{static} \approx 50^\circ$ after immersion into Type-IV deicing fluid for 60 minutes.

Table 2 summarize the measured ice adhesion strengths on the test surfaces before and after immersion into different deicing fluids. It can be seen clearly that, correlating well with its unaffected wettability, the measured ice adhesion strengths on the PTFE coated surfaces were found to be almost unchanged for the test cases before and after being immersed into Type-I deicing fluid, i.e., the differences among the measured ice adhesion data being within the margin of the measurement uncertainty (i.e., being 20 ± 5 kPa). This is believed to be closely related to outstanding anti-corrosive performance of PTFE so that the surface topology and chemistry of the PTFE coated surface would not be changed by Type-I deicing fluid. Therefore, the wettability and the ice adhesion characteristics on the PTFE coated surface were found to be almost unaffected by the immersion of Type-I deicing fluid.

Correlating well with the continuously decreasing droplet contact angles as a function of the immersion time revealed in Fig. 6, the measured ice adhesion strength on the SHS coated surface was found to increase monotonically with the increasing immersion time into Type-I fluid. More specifically, the ice adhesion strength on the SHS coated surface was found to increasing from its original value of $\tau_{ice} \approx 120$ kPa to $\tau_{ice} \approx 390$ kPa after immersion into Type-I deicing fluid for 60 minutes. This may be explained by the facts that, since the SHS coating is solvable to organic solvents according to the information described in its MSDS, the propylene glycol included in Type-I deicing fluid may dissolve a portion of the SHS coating material, thereby, changing the characteristics of the surface roughness/textures on the SHS coated surfaces. As a result, the ice adhesion strength on the SHS coated surface was found to increase about 3.0 times after immersion into Type-I deicing fluid for 60 minutes. The effects of Type-I deicing fluid on the SHS coating will be revealed more clearly from the FTIR and SEM-EDS analysis results to be given in the following section.

Interestingly, the ice adhesion strength on the Enamel coated surface was found to decrease slightly after immersion into Type-I deicing fluid (i.e., decreasing from $\tau_{ice} \approx 1{,}400$ kPa to $\tau_{ice} \approx 1{,}030$ kPa after immersion into Type-I deicing fluid for 60 minutes), which is also consistent with the increasing droplet contact angle on the "contaminated" Enamel coated surface as shown in Fig. 6. The experimental results confirmed the findings reported in the previous studies [62], i.e., the ice adhesion strength on a surface with similar surface roughness/textures would decrease with the increasing droplet contact angle over the surface.

The measurement data given in Table 2 also reveal that, the ice adhesion strengths on both the SHS and PTFE coated surfaces increased substantially after immersion into Type-IV deicing fluid. The measured ice adhesion strength data were found to increase with the immersion duration. After immersion into Type-IV deicing fluid for 60 minutes, while the ice adhesion strengths on the SHS coated surface were found to increase from $\tau_{ice} \approx 120$ kPa to $\tau_{ice} \approx 620$ kPa (i.e., ~ 5.0 times greater), the corresponding value on the PTFE coated surface was found to increase from $\tau_{ice} \approx 20$ kPa to $\tau_{ice} \approx 640$ kPa (i.e., increasing 32 times). It should be noted that the ice adhesion strength on bare aluminum surface was found to be only $\tau_{ice} \approx 450$ kPa as reported in Table 1, which is about 25% lower than those on the SHS or the PTFE coated surfaces after immersion into Type-IV fluid.

In comparison to those on the SHS and PTFE coated surfaces, the effects of Type-IV deicing fluid on the hydrophilic Enamel coating were found to be much trivial. The measured ice adhesion strengths on the Enamel coated surface were found to be almost unchanged (i.e., being about 1400 ± 100 kPa) for the test cases before or after being immersed into Type-IV fluid.

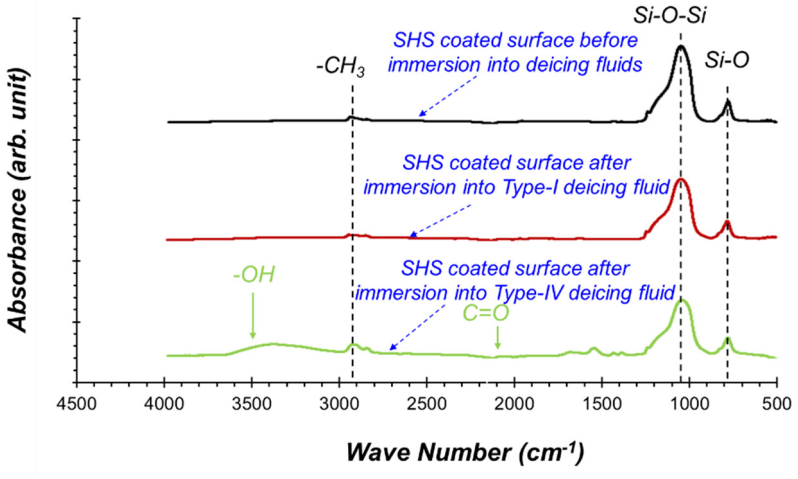

Fig. 8. FTIR analysis results of SHS surface before and after immersion into deicing fluids.

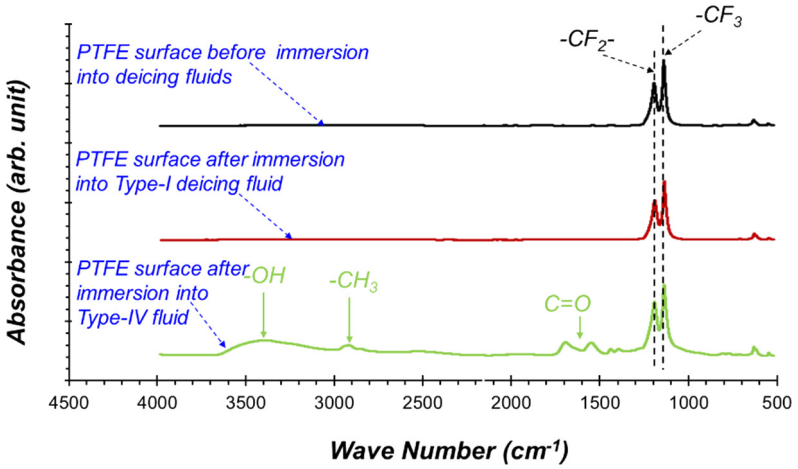

Fig. 9. FTIR analysis results of PTFE surface before and after immersion into deicing fluids.

3.2. FTIR analysis results to characterize various functional groups on the test surfaces

As revealed quantitatively from the surface wettability and ice adhesion strength measurement results given above, both the SHS and PTFE coated surfaces were found to become hydrophilic with the ice adhesion strengths on the test surfaces being increased significantly after immersion in Type-IV deicing fluid. It is well known that, the hydrophobicity of a solid surface is closely related to its surface topology and chemistry characteristics [44]. Therefore, the surface chemistry characteristics of the SHS and PTFE coated surface were examined by using a Fourier-transform infrared spectroscopy (FTIR), which is capable of characterize the functional groups over the test surfaces that are responsible for their hydrophobicity. It is well known that, while some surface functional groups such as the fluorocarbons (e.g., -CF_3 and –CF_2-) are hydrophobic, other surface functional groups including the hydroxyl group (-OH) and the carbonyl group (C=O) are hydrophilic [63]. For a given surface, if the density of the hydrophilic functional groups is greater than that of the hydrophobic functional groups, the surface would become more hydrophilic, and vice versa. Since the focus of the present study is to examine the effects of the deicing fluids on the surface chemistry characteristics of the icephobic coatings (i.e., SHS and PTFE), the FTIR analysis results on the Enamel coated surface will not be discussed in the present study for conciseness.

Fig. 8 and Fig. 9 show the measured FTIR spectra of the SHS and PTFE coated surface before and after being immersed into Type-I and Type-IV deicing fluids. As shown clearly in Fig. 8, the absorbance peaks of Si–O–Si (at 1040 cm^{-1}), Si–O (at 820 cm^{-1}) and –CH_3 (at 2920 cm^{-1}) were found on the SHS coated surface before immersion into the deicing fluids [64]. The absorbance peaks of –CF_3 (at 1200 cm^{-1}) and –CF_2 (at 1150 cm^{-1}) were found to be dominate in the FTIR spectrum of the PTFE coated surface, as revealed in Fig. 9 [63]. Therefore, both SHS and PTFE coated surfaces were found to be hydrophobic due to the existence of the hydrophobic functional groups.

It can also be seen clearly that the FTIR spectra of the SHS and PTFE coated surfaces after immersion into Type-I deicing fluid (i.e., the red curves) were found to be almost the same as those prior to immersion (i.e., the black curves). It suggests that the immersion of the SHS and PTFE coated surfaces into Type-I deicing fluid had little effects on the surface chemistry of the SHS and PTFE coated surface. Therefore, the measured static contact angles of water droplets on the SHS and the PTFE coated test plates were found to be almost unchanged or changed only very slightly after immersion into Type-I deicing fluid, as revealed clearly from the surface wettability measurement results given in Fig. 6.

However, the FTIR spectra of the SHS and PTFE coated surfaces after immersion into Type-IV deicing fluid were found to become significantly different from those prior to immersion. As shown clearly in Fig. 8, a broad peak at 3400 cm^{-1} (-OH groups) was found for the SHS coated surface after immersion into Type-IV

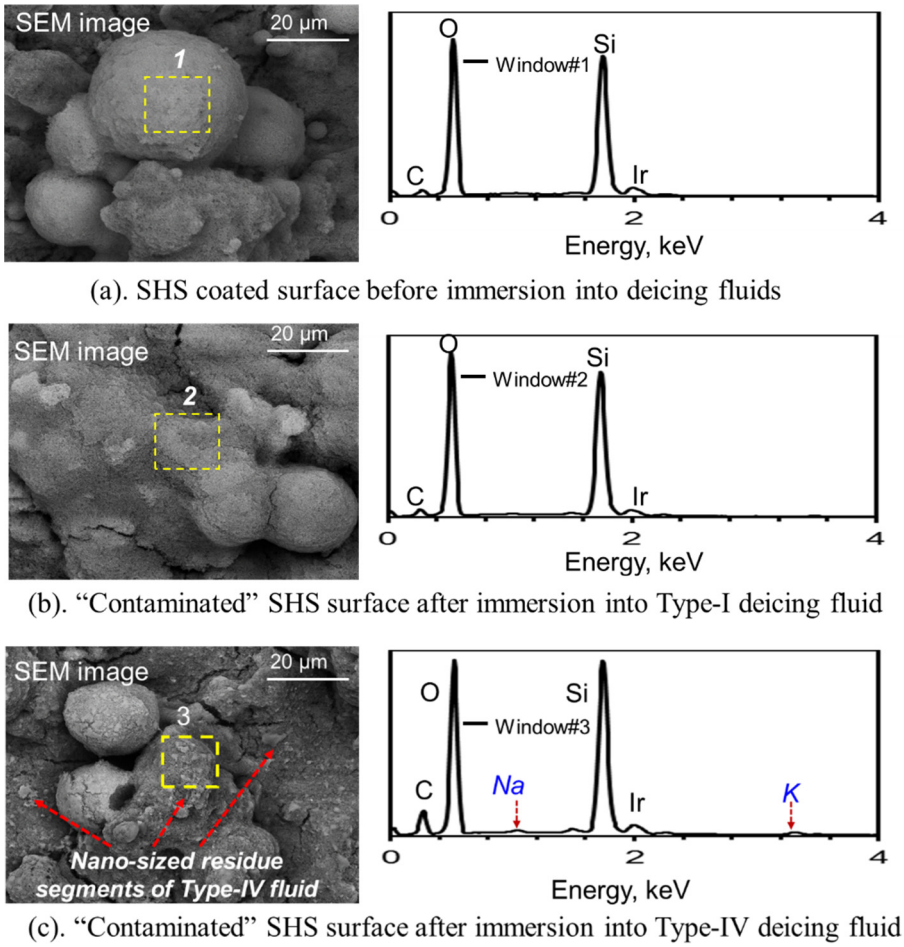

Fig. 10. Acquired SEM images and EDS analysis results of SHS coated surface before and after immersion into Type-I and Type-IV deicing fluids.

deicing fluid. It indicates that, after immersion into Type-IV deicing fluid, abundant hydroxyl groups (-OH) were generated on the SHS coated surface. The hydrophobicity nature of the "clean" SHS coated surface was modified significantly due to the generation of the hydrophilic groups [65]. As a result, the droplet contact angle on the SHS coated surface was found to decrease significantly, i.e., reducing from its original value of $\theta_{static} \approx 156°$ to around only $\theta_{static} \approx 23°$ after immersion into Type-IV deicing fluid for 60 minutes.

As revealed clearly in Fig. 8, obvious absorbance peaks of hydroxyl group (-OH) at 3400 cm^{-1} and hydrophilic carbonyl group (C=O) at 1700 cm^{-1} were also observed on the PTFE coated surface after immersion into Type-IV deicing fluid. The dramatic increase of the hydrophilic functional groups on the surface leads to significant wettability degradation of the PTFE coated surface, i.e., the droplet contact angle was found to decrease from $\theta_{static} \approx 120°$ to only $\theta_{static} \approx 21°$ after immersion into Type-IV fluid for 60 minutes. In summary, since obvious hydrophilic functional groups (i.e., –OH and C=O) were found to be generated on the surfaces, the SHS and the PTFE coated surfaces were found to loss their hydrophobicity and become highly hydrophilic after immersion into Type-IV deicing fluid.

The generation of the hydroxyl and carbonyl groups over the SHS and PTFE coated surfaces after immersion into Type-IV deicing fluid is believed to be attributed by the existence of chemical compound residues of Type-IV deicing fluid on the test surfaces. While Type-IV deicing fluid is composed of ethylene glycol or propylene glycol along with other chemical compounds such as thickening agents, surfactants, corrosion inhibitors, colors and dye [38], some of the chemical compounds have high boiling points (e.g., the boiling point of xanthan gum used as a thickening agent is 311 °C). Therefore, the chemical compounds may not be evaporated completely even though the test plates were dried in a heated vacuum oven at the elevated temperature of 60 °C for over 24 hours. The chemical compound residues of Type-IV deicing fluid remaining on the SHS and PTFE coated surfaces after immersion was confirmed quantitatively based on the SEM and EDS analysis results to be presented in the next section.

3.3. SEM and EDS analysis to characterize the surface topology and elemental composition of the test surfaces before and after immersion into deicing fluids

As aforementioned, a high-resolution SEM system was used in the present study to examine the changes in the surface topology characteristics of the SHS and PTFE coated surface before and after immersion into the deicing fluids. Energy-dispersive X-ray spectroscopy (EDS) analysis was also conducted in the regions of interest on the test surfaces to characterize the material elemental compositions.

Fig. 10 shows the acquired SEM images to reveal the changes in the surface topology of the SHS coated surface before and after immersion into Type-I and Type-IV deicing fluids. Nano-/micro-scaled, hierarchical roughness/textures were clearly observed on the SHS coated surface prior to immersion into deicing fluids, which contribute greatly to the superhydrophobicity of the SHS coated surface. The EDS analysis results at an arbitrarily selected location (i.e., at window #1 indicated in the SEM image) reveal

clearly that the SHS coating is mainly composed of silicon and oxygen elements, which agree well with the independently measured FTIR spectra given in Fig. 8, i.e., Si-O-Si and Si-O are the major functional groups on the SHS coated surface.

As revealed clearly from the SEM image given in Fig. 10(b), in comparison to those over the SHS coated surface prior to immersion, the hierarchical features of the roughness/textures on the SHS coated surface seem to be deteriorated slightly after immersion into Type-I deicing fluid, i.e., the clear boundaries of the hierarchical roughness/textures were found to be smeared. According to the MSDS of the SHS coating used in the present study, since some ingredients of the SHS coating are solvable to organic solvents, the smeared boundaries of the hierarchical roughness/textures on the SHS coated surface after immersion into Type-1 fluid are believed to be caused by the subtle dissolving of the SHS coating materials into the organic solvent included in Type-1 deicing fluid. Since the hierarchical roughness/textures are very important to maintain the superhydrophobicity for a SHS coated surface, the deterioration of the hierarchical features of the SHS surface would cause the wettability degradation. It should also be noted that, even though the hierarchical roughness/textures on the SHS coated surface were found to be deteriorated slightly due to the immersion into Type-I, silicon and oxygen were still found to be the dominant elements on the "contaminated" SHS coated surface, as revealed clearly from the EDS analysis results given in Fig. 10(b). FTIR analysis results given in Fig. 7 also confirmed that Si-O-Si and Si-O were still found to be the major functional groups on the SHS coated surface after immersion into Type-I deicing fluid. Therefore, while the droplet contact angle on the "contaminated" SHS coated surface (i.e., after immersion into Type-I deicing fluid) was found to be reduced slightly (i.e., decreasing from $\theta_{static} \approx 156^{\circ}$ to about $\theta_{static} \approx 148^{\circ}$), the "contaminated" SHS coated surfaces were still found to be almost superhydrophobic since the domination hierarchical features of the surface roughness/textures were found to be unchanged in general.

As revealed clearly from the acquired SEM image given in Fig. 10(c), in addition to the hierarchical surface roughness/textures, many nano-sized structures/segments were also observed on the "contaminated" SHS coated surface. The EDS analysis results clearly reveal that, in additional to Silicon and Oxygen elements which are the chemical components of the SHS coating materials, new chemical elements (i.e., Sodium and Potassium which are originated from the thickening agents and surfactant compounds of Type-IV deicing fluid) were also detected over the "contaminated" SHS coated surface. The EDS measurement results confirm that the nano-sized structures/segments were actually the residues of Type-IV deicing fluid. Since the sizes of the residue segments were found to be much smaller than the hierarchical roughness/textures on the SHS coated surface, the general features of the hierarchical roughness/textures over the "contaminated" SHS coated surface would not be changed due to the existence of the nano-sized residue segments of Type-IV deicing fluid. However, as shown clearly from the FTIR analysis results given in Fig. 8, obvious hydrophilic functional groups (i.e., –OH and C=O) were found to be generated over the "contaminated" SHS surface, which deteriorated the hydrophobicity of the SHS coated surface dramatically. As a result, instead of being superhydrophobic, the SHS surface after immersion into Type-IV fluid was found to become highly hydrophilic due to the existence of the chemical residues of Type-IV fluid on the surface. As a result, the droplet contact angle on the "contaminated" SHS coated surface was found to become $\theta_{static} \approx 23^{\circ}$ after immersion into Type-IV icing fluid for 60 minutes.

Fig. 11 shows the acquired SEM image and EDS analysis results to reveal the variations of the surface topology and chemistry of the PTFE coated surface before and after immersion into the deicing fluids. As revealed clearly from the SEM images, the PTFE coated surface is very porous with intersecting PTFE nanofibers so that water droplets would not be able to penetrate into the nano-sized porous voids easily. Since PTFE material itself is hydrophobic and has extremely low surface energy [43], the ice adhesion on the PTFE coated surface prior to immersion into deicing fluids was found to be ultra-low (i.e., $\tau_{ice} \approx 20$ kPa), in comparison to that on the uncoated aluminum surface ($\tau_{ice} \approx 450$ kPa) or Enamel coated surface (i.e., $\tau_{ice} \approx 1{,}400$ kPa). The EDS analysis results given in Fig. 11 reveal that the PTFE coated surface contains mainly carbon and fluorine elements, which agrees well with the measurement results of the FTIR analysis results given in Fig. 7 (i.e., functional groups of $-CF_2$ and $-CF_3$ were identified on the PTFE surface). Due to the outstanding anti-corrosive performance of PTFE material, both the surface topology and the elemental compositions of the PTFE coated surface were found to be almost unaffected by Type-I deicing fluid. Therefore, the measured droplet contact angle and ice adhesion strength of the PTFE surface were found to be almost unchanged for the test cases before and after immersion into Type-I deicing fluid. However, as revealed clearly from the SEM image given in Fig. 11(c), residues of Type-IV deicing fluid were observed on the "contaminated" PTFE surface. The EDS analysis results given in Fig. 11(c) also confirm that, while Sodium and Potassium elements were detected in selected Window #4 indicated in the SEM image which is believed to be the area covered by the residues of Type-IV deicing fluid. However, neither Sodium nor Potassium was not detected in Window #3, which is apparently the "clean" PTFE surface without any residues of Type-IV deicing fluid. Due to the existence of Type-IV deicing fluid residues, the "contaminated" PTFE surface was found to become highly hydrophilic with the droplet contact angle becoming $\theta_{static} \approx 22^{\circ}$. Since the residues of Type-IV deicing fluid would make the test surface becoming highly hydrophilic, water droplets on the "contaminated" PTFE surface would be more readily to penetrate into the voids between the intersecting PTFE porous nanofibers. As the water inside the voids between the intersecting PTFE porous fibers is frozen into ice, the ice adhesion strength on the "contaminated" PTFE surface would become much stronger due to the interlocking between ice and the surface textures [30]. As a result, the ice adhesion strength on the "contaminated" PTFE surface were found to increase significantly after immersion into Type-IV deicing fluid, as reported in Table 2.

3.4. Ice accretion experiments to compare the ice accretion characteristics on the icephobic coated airfoil models before and after immersion into the deicing fluids

By leveraging the unique ISU-IRT, an experimental campaign was also conducted to compare the ice accretion characteristics over the surfaces of SHS and PTFE coated airfoil/wing models before and after immersion into different deicing fluids in order the demonstrate the detrimental effects of the deicing fluids on the performance of the icephobic coatings for icing mitigation. In performing the ice accretion experiments, ISU-IRT was operated at a pre-scribed frozen-cold temperature level (i.e., $T_{\infty} = -5.0\,^{\circ}\mathrm{C}$ for the present study) for at least 20 min to ensure ISU-IRT reaching a thermal steady state. Since the temperature inside ISU-IRT was set to be well below the water frozen temperature, the water droplets exhausted from the spray nozzles/atomizers would be in a supercooled state after exhausted from the water spray system. Ice accretion process would start immediately as the super-cooled water droplets impacting onto the airfoil/wing models. For all the test cases of the present study, the incoming airflow velocity, temperature, liquid water content (*LWC*) level in ISU-IRT were set to be $V_{\infty} = 40$ m/s; $T_{\infty} = -5.0\,^{\circ}\mathrm{C}$; and $LWC = 2.0$ g/m^3, respectively. Based on the work of Liu and Hu [66], the ice accretion processes over the surfaces of the airfoil/wing models installed in ISU-IRT are

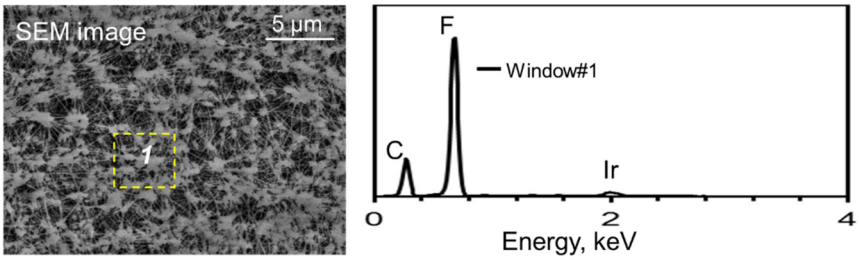

(a). PTFE coated surface before immersion into deicing fluids

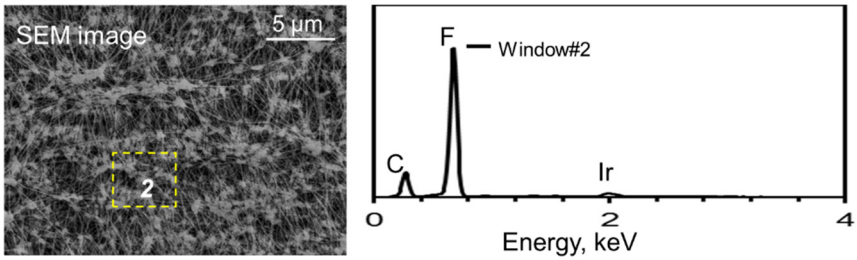

(b). "Contaminated" PTFE surface after immersion into Type-I deicing fluid

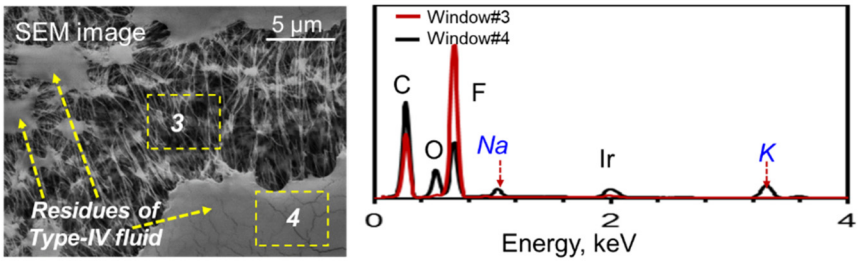

(c). "Contaminated" PTFE surface after immersion into Type-IV deicing fluid

Fig. 11. Acquired SEM images and EDS analysis results of the PFTE surface before and after immersion into Type-I and Type-IV deicing fluids.

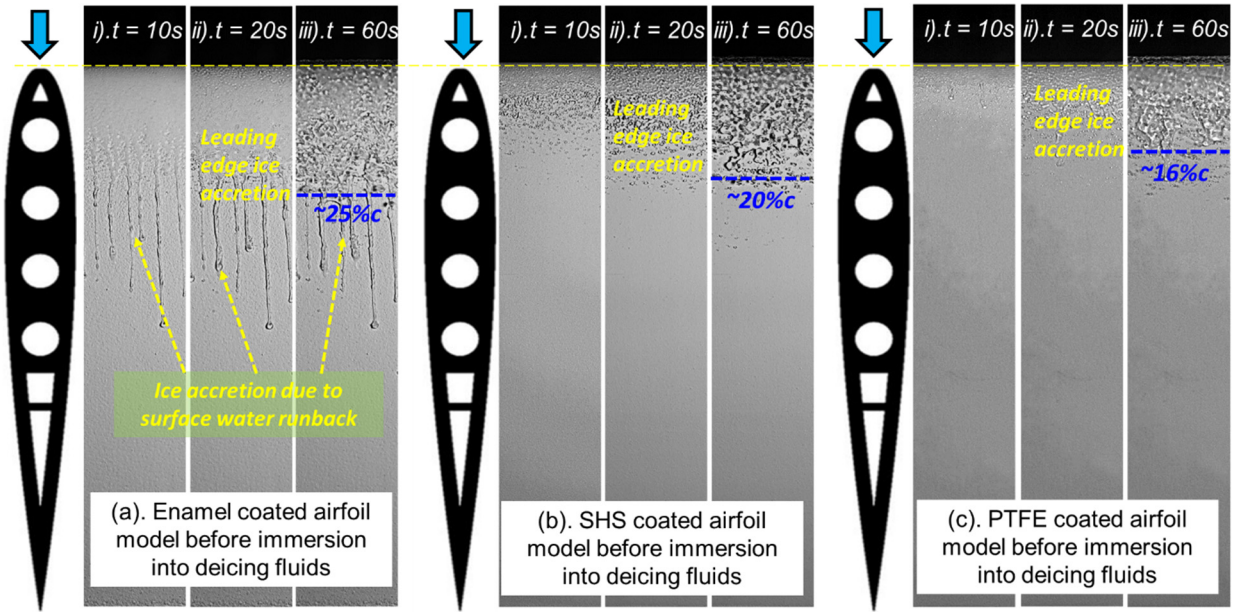

Fig. 12. Acquired images to reveal the dynamic ice accretion processes on the airfoil/wing models coated with different coatings before immersion into deicing fluids.

expected to be of typical glaze icing process under the icing test conditions used in the present study.

Fig. 12 gives typical snapshots of acquired images to reveal the dynamic ice accretion processes over the surfaces of the airfoil/wing models coated with the icephobic coatings (i.e., SHS and PTFE) prior to immersion into deicing fluids. The ice accretion images on the airfoil/wing model coated with hydrophilic Enamel coating were also given in Fig. 12 as the comparison baseline to demonstrate the effectiveness of using icephobic coatings for aircraft inflight icing mitigation. As shown clearly in Fig. 12(a), with

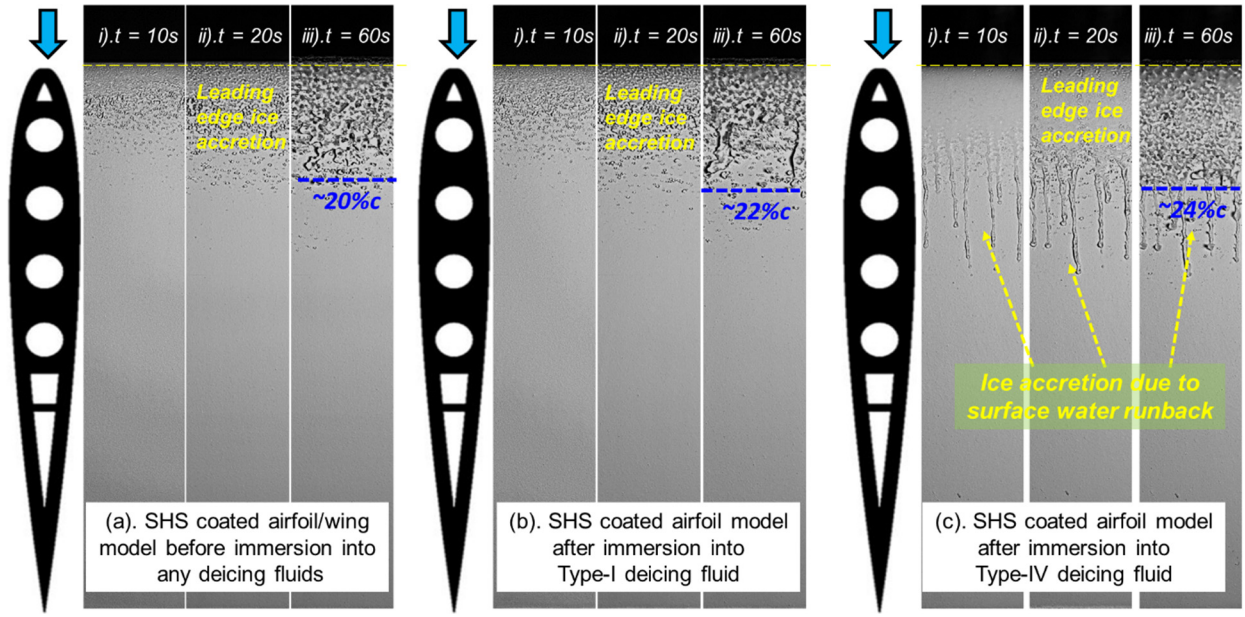

Fig. 13. Acquired images to reveal the changes of the dynamic ice accretion processes over the SHS coated airfoil surface before and after immersion into Type-I and Type-IV deicing fluids.

the airfoil surface being hydrophilic (i.e., for the scenario with Enamel coated surface or uncoated aluminum-alloy surface), ice was found to accrete rapidly on the surface of the airfoil model, upon impacting of super-cooled water droplets carried by the incoming frozen-cold airflow. Similar as that described by Liu and Hu [66], due to the inadequate heat transfer to remove/dissipate all the released latent heat of fusion associated with the solidification (i.e., icing process) under the wet glaze icing conditions used in the present study, only a portion of the impacted supercooled water droplets would be frozen into ice instantly, while the rest of the impacted water mass would stay in liquid and accumulate over the airfoil front surface. As driven by the boundary layer airflow over the airfoil surface, the unfrozen surface water collected near the airfoil leading edge was found to run back to form multiple water rivulets over the downstream airfoil surface to transport the surface water collected near the airfoil leading edge to further downstream locations [67]. Since the ambient airflow was set to be well below the water frozen temperature (i.e., $T_\infty = -5.0\,°C$), the runback surface water was found to be frozen into ice eventually to form rivulet-shaped ice structures at further downstream locations, as shown clearly in Fig. 12(a).

It can also be seen clearly that, after applying the icephobic coatings (i.e., both SHS and PTFE coatings) to cover the surfaces of the airfoil/wing models, the ice accretion over the icephobic airfoil surfaces of the test models was found to be suppressed substantially, in comparison to that over the hydrophilic airfoil surface. In addition to having smaller coverages of the ice layers accreted near the airfoil leading edge (i.e., due to the direct impinging of the supercooled water droplets), almost no traces of the water runback or rivulet-shaped ice structures were observed on the icephobic coated airfoil surfaces. The effectiveness of using the icephobic coatings (i.e., both SHS and PTFE) for aircraft icing mitigation was demonstrated clearly based on the side-by-side comparison of the ice accretion images given in Fig. 12. As suggested in Zhang et al. [30], the much less ice accretion on the SHS and PTFE coated airfoil surfaces is mainly due to following two reasons: The much slippery nature (i.e., less capillary forces associated with the bigger droplet contact angles) of the hydrophobic SHS and PTFE surfaces would enable the impacted supercooled water droplets to become more easily bouncing off and/or rolling away from the airfoil surfaces before being frozen into ice. In addition, the much smaller ice adhesion strengths on the icephobic surfaces would also enable the aerodynamic shear forces exerted by the incoming airflow to be more readily to sweep away the accreted ice structures from the airfoil surfaces. It can also be seen that, corresponding to the much weaker ice adhesion strength on the PFTE surface in comparison to that on the SHS surface (i.e., $\tau_{ice} \approx 20$ kPa on PTFE surface vs. $\tau_{ice} \approx 120$ kPa on SHS surface), the coverage of the ice layer accreted near the airfoil leading edge over the PTFE coated airfoil surface was found to be noticeably smaller than that on the SHS coated airfoil surface. More specifically, after 60 seconds of the ice accretion experiment, while the ice layer accreted on the airfoil front surface was found to reach to the downstream location of $X/C \approx 20\%$ on the SHS coated airfoil model, the corresponding value was found to be only $X/C \approx 16\%$ on the PTFE coated airfoil surface. In comparison, the coverage of the ice layer accreted over the airfoil front surface was found to extend to the downstream location of $X/C \approx 25\%$ on the hydrophilic Enamel coated airfoil surface.

Fig. 13 shows the variations of the dynamic ice accretion process on the SHS coated airfoil/wing models before and after immersion into deicing fluids under the same icing conditions of $V_\infty = 40$ m/s; $T_\infty = -5.0\,°C$; and $LWC = 2.0$ g/m^3. It can be seen clearly that, since the surface wettability and ice adhesion characteristics of the SHS surface were found to be deteriorated slightly after immersion into Type-1 deicing fluid (i.e., while the droplet contact angle decreases from $\theta_{static} \approx 156°$ to $\theta_{static} \approx 148°$, corresponding ice adhesion strength increases from $\tau_{ice} \approx 120$ kPa to $\tau_{ice} \approx 390$ kPa), the ice structures accreted on the SHS coated airfoil surface was found to increase slightly after immersion into Type-I deicing (i.e., the ice layer accreted over airfoil front surface was found to extend to the downstream location of $X/C \approx 22\%$ after 60 seconds of the ice accretion experiment, instead of the original value $X/C \approx 20\%$ for the case prior to immersion. It should also be noted, since the effects of Type-I deicing fluid on the wettability of the SHS coated surface is very minor (i.e., smearing the hierarchical surface roughness/textures on the SHS surface slightly as shown in the SEM image given in Fig. 10), the droplet contact angles on the "contaminated" SHS coated surfaces were still found to be very large (i.e., $\theta_{static} \approx 148°$), indicating that the "contaminated" SHS surface was still almost superhydrophobic due to the remaining general features of the hierarchical surface rough-

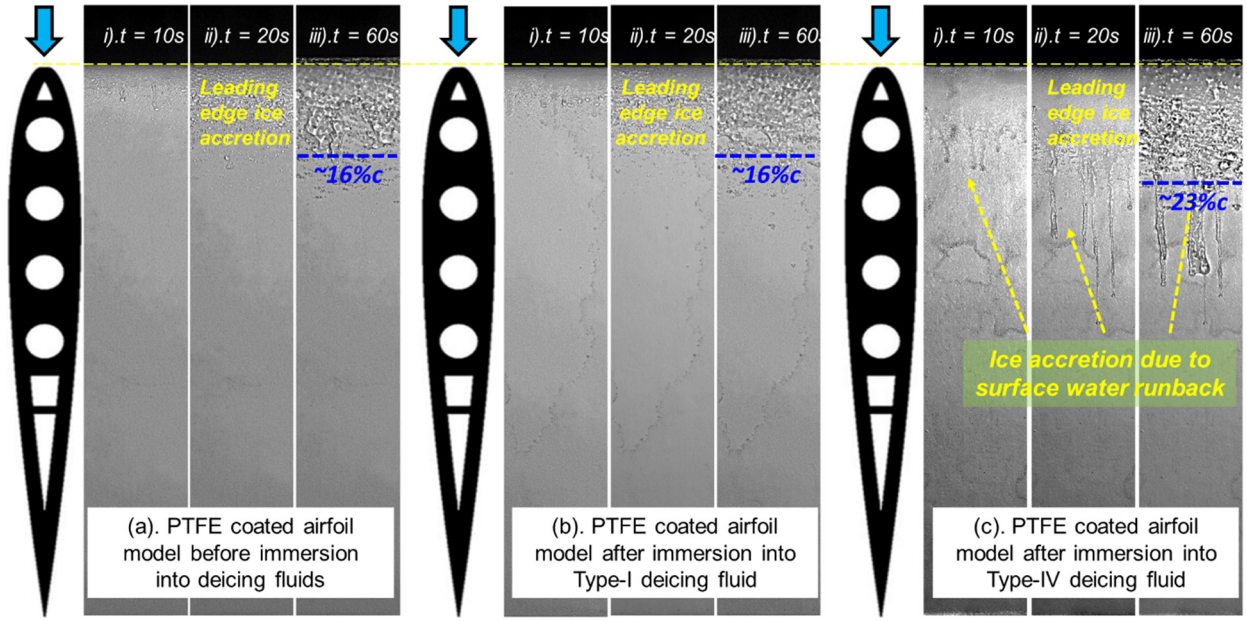

Fig. 14. Acquired images to reveal the dynamic ice accretion process on the PTFE coated airfoil/wing models before and after immersion into Type-I and Type-IV deicing fluids.

ness/textures. As a result, the impacted water droplets would still run back swiftly and shed away from the airfoil surface quickly before being frozen into ice [30]. Therefore, no rivulet-shaped ice structures were observed on the SHS coated airfoil surface even after being "contaminated" by Type-1 deicing fluid, as shown in Fig. 13(b).

As revealed clearly from the ice accretion images given in Fig. 13(c), the ice accretion process over the SHS coated airfoil surface after immersion into Type-IV deicing fluid was found to be significantly different from the other two compared cases. In addition to having a larger coverage of the ice layer accreted over the fount airfoil surface (i.e., extending to the downstream location of $X/C \approx 24\%$ after 60 seconds of ice accretion experiment), multiple rivulet-shaped ice structures were found to be formed on the further downstream of the airfoil surface, which is very similar as those accreted over the hydrophilic airfoil surface given in Fig. 12(a). The significant increase of the ice accretion on the SHS coated airfoil surface after immersion into Type-IV deicing fluid is believed to be closely related to the dramatic detrimental effects of Type-IV deicing fluid on the surface wettability and ice adhesion characteristics of the SHS coated surface. As discussed above, due to the existence of chemical compound residues of Type-IV fluid on the SHS coated surface, while the "contaminated" SHS surface was found to change dramatically from being superhydrophobic to highly hydrophilic (i.e., droplet contact angle *decreasing from* $\theta_{static} \approx 156°$ to only $\theta_{static} \approx 23°$ after being contaminated by Type-IV deicing fluid), the ice adhesion strength of the "contaminated" SHS surface was also found to increase significantly (i.e., increasing from $\tau_{ice} \approx 120$ kPa to $\tau_{ice} \approx 620$ kPa, correspondingly). Therefore, after being "contaminated" by Type-IV deicing fluid, the ice accretion process on the SHS coated airfoil surface were found to become very similar as that on the Enamel coated airfoil surface with obvious traces of water runback and formation of rivulet-shaped ice structures on the further downstream surface of the airfoil/wing model.

Fig. 14 presents the acquired images of the ice accretion process on the PTFE coated airfoil/wing models before and after immersion into the deicing fluids, which reveal the effects of the deicing fluids on the effectiveness of the PTFE coating for aircraft icing mitigation clearly. As described above, since the surface wettability and ice adhesion characteristics on the PFTE coated surface would not be affected by the immersion operation into Type-1 deicing fluid due to the outstanding anti-corrosive performance of the PTFE material, the characteristics of the ice accretion process on the PTFE coated surface were found to be almost identical before and after immersion into Type-I deicing fluid. However, after immersion into Type-IV deicing fluid, the chemical compound residues of Type-IV deicing fluid remaining on the PTFE coated surface would make the "contaminated" PTFE surface becoming highly hydrophilic (i.e., $\theta_{static} \approx 22°$) and ice adhesion strength increasing significantly (i.e., $\tau_{ice} \approx 650$ kPa). Therefore, while the ice layer accreted over the airfoil front surface was found to extend to further downstream location of $X/C \approx 23\%$ after 60 seconds of ice accretion experiment, multiple rivulet-shaped ice structures were also observed on the further downstream locations of the PTFE surface after being "contaminated by Type-IV deicing fluid, as shown clearly in Fig. 14(c).

4. Conclusions

An experimental investigation was conducted to study the implications/effects of spraying deicing fluids to airframe surface for aircraft ground deicing on the performance of icephobic coatings applied over the airframe surfaces for aircraft inflight icing mitigation. While two kinds of icephobic coatings, i.e., a superhydrophobic surface (SHS) coating and a polytetrafluoroethylene (PTFE) coating, were selected for the present study, a general industrial-used Enamel coating was used as the comparison baseline in the present study. Test plates and airfoil/wing models with their surfaces treated with different coatings (i.e., SHS, PTFE and Enamel) were prepared for a comparative study. The test plates and airfoil models were first immersed into containers filled with two typical deicing fluids (i.e., Newtonian Type-I fluid and Non-Newtonian Type-IV fluid) to simulate the scenario of spraying a layer of deicing fluid onto the airframe surface for aircraft ground deicing operation. After immersion into the deicing fluids with pre-selected durations (i.e., up to 60 minutes), the test plates and airfoil models were placed on an inclined bench to drain off the deicing fluids for 48 hours, and then put into a heated vacuum oven at an elevated temperature of 60 °C for 24 hours to dry out the liquids remaining on the test surfaces. Such a procedure is designed to simulate the runoff all the deicing fluids from airframe surfaces as airplanes take off from airports. The changes of the surface wettability (i.e.,

in the term of the droplet contact angles, θ_{static}) and ice adhesion strengthen on the test plates treated with different coatings were characterized before and after they were immersed into the deicing fluids in order to quantify the performance degradation of the icephobic coatings due to the immersion into the deicing fluids. Advanced diagnostic systems, including scanning electron microscopy (SEM), Fourier transformed infrared spectroscopy (FTIR) and energy dispersive X-ray spectroscopy (EDS), were used to characterize the changes in the surface topology and chemistry of the icephobic coatings before and after immersion into the deicing fluids. By leveraging the icing research tunnel available at Iowa State University, an icing experiment campaign was also conducted to demonstrate the detrimental effects of deicing fluids on the effectiveness of using the icephobic coatings to mitigate/suppress ice accretion on airfoil/wing surfaces.

It was found that Type-I deicing fluid has very limited effects on the performance of icephobic coatings for aircraft icing mitigation. Based on the FTIR and EDS analysis results, it was confirmed that no chemical compounds of Type-I deicing fluid would remain on the SHS or PTFE coated surfaces after Type-1 deicing fluid was drained off from the test surfaces. The acquired SEM images revealed clearly that immersion of the SHS coated surface into Type-1 deicing fluid would cause smearing of the hierarchical roughness/textures over the SHS surface, possibly due to a weak dissolution of the SHS coating material into Type-1 deicing fluid. As a result, while the wettability of the SHS surface was found to be deteriorated slightly, and the resultant ice adhesion strength was found to increase substantially. More specifically, while the droplet contact angle on the SHS coated surface was found to reduce from $\theta_{static} \approx 156^\circ$ to $\theta_{static} \approx 148^\circ$ after immersion into Type-I deicing fluid for 60 minutes, the ice adhesion strength increased from $\tau_{ice} \approx 120$ kPa to $\tau_{ice} \approx 390$ kPa, correspondingly. The ice accretion experiments confirmed that the SHS coating became slightly less effective to mitigate/suppress ice accretion on the airfoil/wing model after immersion into Type-1 deicing fluid, which correlated well the degradations of the surface wettability and ice adhesion characteristics induced by Type-I deicing fluid. Due to the outstanding anti-corrosive performance of PTFE material, Type-1 deicing fluid was found to have almost no effects on the surface wettability and ice adhesion characteristics of the PTFE coated surface. The ice accretion experiments also confirmed that the dynamic ice accretion process over PTFE coated airfoil surface as found to be unchanged before and after immersion into Type-1 deicing fluid.

However, Type-IV deicing fluid was found to deteriorate the anti-icing performance of icephobic coatings (i.e., both SHS and PTFE) significantly. Both the FTIR and EDS analysis results confirmed that some of the chemical compounds of Type-IV deicing fluid (e.g., Sodium and Potassium elements) would remain on the test surfaces even though Type-IV deicing fluid was drained off from the icephobic coated surfaces. The residues of Type-IV deicing fluid on the icephobic coated surfaces were also observed clearly as nano-scaled fragments/structures in the acquired SEM images. The chemical residual compounds remaining on the SHS and PTFE surfaces were found to cause the generation of various hydrophilic groups (e.g., hydroxyl group (-OH) and carbonyl group (C=O)) over the test surfaces, which make the "contaminated" test surfaces changing from hydrophobic to highly hydrophilic. More specifically, after immersion into Type-IV deicing fluid for 60 minutes, while the measured droplet contact angle on the "contaminated" SHS surface was found to reduce from $\theta_{static} \approx 156^\circ$ to $\theta_{static} \approx 23^\circ$, the corresponding value decreased from $\theta_{static} \approx 120^\circ$ to $\theta_{static} \approx 22^\circ$ on the PTFE coated surface. Meanwhile, the ice adhesion strength on the "contaminated" SHS surface was found to increase over 5.0 times (i.e., increasing from $\tau_{ice} \approx 120$ kPa to $\tau_{ice} \approx 620$ kPa), the measured values on the PTFE coated surface increased over 30 times (i.e., increasing from $\tau_{ice} \approx 20$ kPa to $\tau_{ice} \approx 640$ kPa) after immersion into. The ice accretion experiments also demonstrated clearly that the "contamination" of Type-IV deicing fluid to the icephobic coatings (i.e., both SHS and PTFE coatings) would deteriorate their effectiveness for aircraft icing mitigation dramatically.

In summary, the research findings of the present study suggested that, spraying Type-1 deicing fluid over airframe surfaces for aircraft ground deicing operation would have very little or almost no effects on the performance of the icephobic coatings for aircraft inflight icing mitigation. However, spraying Type-IV deicing fluid over airframe surfaces for aircraft ground deicing would result in significant "contaminations" to the icephobic coatings (i.e., for both SHS and PTFE coatings) on the aircraft surfaces, which would deteriorate their effectiveness to suppress/mitigate ice accretion over airframe surfaces dramatically.

Declaration of competing interest

The authors declare that they have no known competing financial interests or personal relationships that could have appeared to influence the work reported in this paper.

Acknowledgements

The research work is partially supported by Iowa Space Grant Consortium (ISGC) Base Program for Aircraft Icing Studies under award number 422-20-81, and National Science Foundation (NSF) under award numbers of CMMI-1824840 and CBET-1916380. Cryotech Deicing Technology Company is acknowledged for providing deicing fluids used for the present study. The authors want to thank Dapeng Jing and Warren Straszheim of Iowa State University for their help in conducting SEM-EDS analysis.

References

[1] D.I. Ignatyev, A.N. Khrabrov, A.I. Kortukova, D.A. Alieva, M.E. Sidoryuk, S.G. Bazhenov, Interplay of unsteady aerodynamics and flight dynamics of transport aircraft in icing conditions, Aerosp. Sci. Technol. 104 (2020) 105914, https://doi.org/10.1016/j.ast.2020.105914.

[2] X. Huang, N. Tepylo, V. Pommier-Budinger, M. Budinger, E. Bonaccurso, P. Villedieu, L. Bennani, A survey of icephobic coatings and their potential use in a hybrid coating/active ice protection system for aerospace applications, Prog. Aerosp. Sci. 105 (2019) 74–97, https://doi.org/10.1016/j.paerosci.2019.01.002.

[3] T. Cebeci, F. Kafyeke, Aircraft icing, Annu. Rev. Fluid Mech. 35 (2003) 11–21, https://doi.org/10.1146/annurev.fluid.35.101101.161217.

[4] F. Mosher, D. Schaum, C. Herbster, T. Guinn, Analysis of causes of icing conditions which contributed to the crash of continental flight 3407, in: 14th Conf. Aviat. Range, Aerosp. Meteorol., 2010, http://commons.erau.edu/db-applied-aviation/21/. (Accessed 11 February 2016).

[5] D.J. Haase, Aircraft ground deicing, a flight crew perspective, J. Aircr. 30 (1993) 19–23, https://doi.org/10.2514/3.56877.

[6] H. Coffman Jr., Review of helicopter icing protection systems, in: Aircr. Des. Syst. Technol. Meet., 1983.

[7] Y. Cao, W. Tan, Z. Wu, Aircraft icing: an ongoing threat to aviation safety, Aerosp. Sci. Technol. 75 (2018) 353–385, https://doi.org/10.1016/j.ast.2017.12.028.

[8] S.K. Thomas, R.P. Cassoni, C.D. MacArthur, Aircraft anti-icing and de-icing techniques and modeling, J. Aircr. 33 (1996) 841–854, https://doi.org/10.2514/3.47027.

[9] O. Parent, A. Ilinca, Anti-icing and de-icing techniques for wind turbines: critical review, Cold Reg. Sci. Technol. 65 (2011) 88–96, https://doi.org/10.1016/j.coldregions.2010.01.005.

[10] L. Gray, Review of aircraft deicing and anti-icing fluid storm water runoff control technologies, in: MANE 6960H01 – Air and Water Pollution Prevention, 2013, http://www.ewp.rpi.edu/hartford/~grayl3/AWPPCE/Water/Project/Aircraft De-icing Effluent Control Methods-Gray.pdf. (Accessed 14 February 2016).

[11] Y. Lin, H. Chen, G. Wang, A. Liu, Recent progress in preparation and anti-icing applications of superhydrophobic coatings, Coatings 8 (2018) 208, https://doi.org/10.3390/coatings8060208.

[12] S.K. Thomas, R.P. Cassoni, C.D. MacArthur, Aircraft anti-icing and de-icing techniques and modeling, J. Aircr. 33 (5) (2012) 841–854, http://arc.aiaa.org/doi/abs/10.2514/3.47027. (Accessed 14 February 2016).

[13] S.K. Jung, L.P. Raj, A. Rahimi, H. Jeong, R.S. Myong, Performance evaluation of electrothermal anti-icing systems for a rotorcraft engine air intake using a meta model, Aerosp. Sci. Technol. 106 (2020) 106174, https://doi.org/10.1016/j.ast.2020.106174.

[14] C. Kolbakir, H. Hu, Y. Liu, H. Hu, An experimental study on different plasma actuator layouts for aircraft icing mitigation, Aerosp. Sci. Technol. 107 (2020) 106325, https://doi.org/10.1016/j.ast.2020.106325.

[15] L. Li, Y. Liu, L. Tian, H. Hu, H. Hu, X. Liu, I. Hogate, A. Kohli, An experimental study on a hot-air-based anti-/de-icing system for aero-engine inlet guide vanes, Appl. Therm. Eng. 167 (2020) 114778, https://doi.org/10.1016/j.applthermaleng.2019.114778.

[16] L. Ma, Z. Zhang, L. Gao, Y. Liu, H. Hu, Bio-inspired icephobic coatings for aircraft icing mitigation: a critical review, Rev. Adhes. Adhes. 8 (2020) 168–199, https://doi.org/10.7569/RAA.2020.097307.

[17] Y.H. Yeong, A. Milionis, E. Loth, J. Sokhey, Self-lubricating icephobic elastomer coating (SLIC) for ultralow ice adhesion with enhanced durability, Cold Reg. Sci. Technol. 148 (2018) 29–37, https://doi.org/10.1016/j.coldregions.2018.01.005.

[18] Y. Cheng, D. Rodak, C. Wong, C. Hayden, Effects of micro-and nanostructures on the self-cleaning behaviour of lotus leaves, Nanotechnology 17 (2006) 1359–1362, http://iopscience.iop.org/article/10.1088/0957-4484/17/5/032/meta. (Accessed 14 February 2016).

[19] K. Koch, B. Bhushan, Y. Jung, W. Barthlott, Fabrication of artificial Lotus leaves and significance of hierarchical structure for superhydrophobicity and low adhesion, Soft Matter 5 (2009) 1386–1393, http://pubs.rsc.org/en/content/articlehtml/2009/sm/b818940d. (Accessed 14 February 2016).

[20] J. Chen, R. Dou, D. Cui, Q. Zhang, Y. Zhang, F. Xu, X. Zhou, J. Wang, Y. Song, L. Jiang, Robust prototypical anti-icing coatings with a self-lubricating liquid water layer between ice and substrate, ACS Appl. Mater. Interfaces 5 (2013) 130510105547001, https://doi.org/10.1021/am401004t.

[21] L. Mishchenko, B. Hatton, V. Bahadur, Design of ice-free nanostructured surfaces based on repulsion of impacting water droplets, ACS Nano 4 (12) (2010) 7699–7707, http://pubs.acs.org/doi/abs/10.1021/nn102557p. (Accessed 14 February 2016).

[22] C. Antonini, F. Villa, M. Marengo, Oblique impacts of water drops onto hydrophobic and superhydrophobic surfaces: outcomes, timing, and rebound maps, Exp. Fluids 55 (2014) 1713, https://doi.org/10.1007/s00348-014-1713-9.

[23] A. Meuler, G. McKinley, R. Cohen, Exploiting topographical texture to impart icephobicity, ACS Nano 4 (2010) 7048–7052, http://pubs.acs.org/doi/abs/10.1021/nn103214q. (Accessed 14 February 2016).

[24] A. Cassie, S. Baxter, Wettability of porous surfaces, Trans. Faraday Soc. 40 (1944) 546–551, http://pubs.rsc.org/en/content/articlepdf/1944/tf/tf9444000546. (Accessed 14 February 2016).

[25] L. Cao, A.K. Jones, V.K. Sikka, J. Wu, D. Gao, Anti-icing superhydrophobic coatings, Langmuir 25 (2009) 12444–12448, https://doi.org/10.1021/la902882b.

[26] Z.J. Wang, D.J. Kwon, K. Lawrence DeVries, J.M. Park, Frost formation and anti-icing performance of a hydrophobic coating on aluminum, Exp. Therm. Fluid Sci. 60 (2015) 132–137, https://doi.org/10.1016/j.expthermflusci.2014.09.003.

[27] R.M. Waldman, H. Hu, High-speed imaging to quantify transient ice accretion process over an airfoil, J. Aircr. 53 (2015) 369–377, https://doi.org/10.2514/1.C033367.

[28] Y. Liu, L. Li, H. Li, H. Hu, An experimental study of surface wettability effects on dynamic ice accretion process over an UAS propeller model, Aerosp. Sci. Technol. 73 (2018) 164–172, https://doi.org/10.1016/j.ast.2017.12.003.

[29] L. Gao, Y. Liu, L. Ma, H. Hu, A hybrid strategy combining minimized leading-edge electric-heating and superhydro-/ice-phobic surface coating for wind turbine icing mitigation, Renew. Energy 140 (2019) 943–956, https://doi.org/10.1016/J.RENENE.2019.03.112.

[30] Z. Zhang, L. Ma, Y. Liu, J. Ren, H. Hu, An experimental study of rain erosion effects on a hydro-/ice-phobic coating pertinent to Unmanned-Arial-System (UAS) inflight icing mitigation, Cold Reg. Sci. Technol. 181 (2021) 103196, https://doi.org/10.1016/j.coldregions.2020.103196.

[31] C. (Chris) Qin, A.T. Mulroney, M.C. Gupta, Anti-icing epoxy resin surface modified by spray coating of PTFE Teflon particles for wind turbine blades, Mater. Today Commun. 22 (2020) 100770, https://doi.org/10.1016/j.mtcomm.2019.100770.

[32] R. Menini, M. Farzaneh, Advanced icephobic coatings, J. Adhes. Sci. Technol. 25 (2011) 971–992, https://doi.org/10.1163/016942410X533372.

[33] P.J. Rivero, R.J. Rodriguez, S. Larumbe, M. Monteserín, F. Martín, A. García, C. Acosta, M.J. Clemente, P. García, J. Mora, A. Agüero, Evaluation of functionalized coatings for the prevention of ice accretion by using icing wind tunnel tests, Coatings 10 (2020) 636, https://doi.org/10.3390/coatings10070636.

[34] Q. Chao, L. Meng, C. Shuxian, Anti-icing characteristics of PTFE super hydrophobic coating on titanium alloy surface, J. Alloys Compd. 860 (2021) 157907, https://doi.org/10.1016/j.jallcom.2020.157907.

[35] Y. Yu, L. Chen, D. Weng, J. Wang, C. Chen, A. Mahmood, A promising self-assembly PTFE coating for effective large-scale deicing, Prog. Org. Coat. 147 (2020) 105732, https://doi.org/10.1016/j.porgcoat.2020.105732.

[36] E.G. Hill, T.A. Zierten, Aerodynamic effects of aircraft ground deicing/anti-icing fluids, J. Aircr. 30 (1993) 24–34, https://doi.org/10.2514/3.46301.

[37] P. Koivisto, T. Honkanen, M. Auvinen, A. Hellsten, K. Kahma, De-icing fluid flow-off from a flat plate in an accelerating airstream, AIAA J. 58 (2020) 1607–1619, https://doi.org/10.2514/1.J058706.

[38] Y. Wang, N.E. Hudson, R.A. Pethrick, C.J. Schaschke, Poly(acrylic acid)-poly(vinyl pyrrolidone)-thickened water/glycol de-icing fluids, Cold Reg. Sci. Technol. 101 (2014) 24–30, https://doi.org/10.1016/j.coldregions.2014.01.006.

[39] P. Koivisto, E. Soinne, J. Kivekäs, Anti-icing fluid secondary wave and its role in lift loss during takeoff, J. Aircr. 55 (2018) 2298–2306, https://doi.org/10.2514/1.c034694.

[40] A.P. Broeren, J.T. Riley, Review of the Aerodynamic Acceptance Test and Application to Anti-Icing Fluids Testing in the NRC Propulsion and Icing, Wind Tunnel, Cleveland, 2012.

[41] A.P. Broeren, S. Lee, C. Clark, Aerodynamic effects of anti-icing fluids on a thin high-performance wing section, J. Aircr. 53 (2015) 451–462, https://doi.org/10.2514/1.c033384.

[42] E. Villeneuve, J.-D. Brassard, C. Volat, Effect of various surface coatings on de-icing/anti-icing fluids aerodynamic and endurance time performances, Aerospace 6 (2019) 114, https://doi.org/10.3390/aerospace6100114.

[43] Q. Chao, L. Meng, C. Shuxian, Anti-icing characteristics of PTFE super hydrophobic coating on titanium alloy surface, J. Alloys Compd. 860 (2021) 1579071.

[44] J.T. Simpson, S.R. Hunter, T. Aytug, Superhydrophobic materials and coatings: a review, Rep. Prog. Phys. 78 (2015), https://doi.org/10.1088/0034-4885/78/8/086501.

[45] L.Q. Ma, Z.C. Zhang, L.Y. Gao, Y. Liu, H. Hu, An exploratory study on using Slippery-Liquid-Infused-Porous-Surface (SLIPS) for wind turbine icing mitigation, Renew. Energy 162 (2020) 2344–2360.

[46] L. Gao, Y. Liu, H. Hu, Quantification of dynamic glaze icing process over an airfoil surface by using a digital image projection (DIP) technique, in: 2018 Atmos. Sp. Environ. Conf., 2018, pp. 1–13.

[47] J.T. Korhonen, T. Huhtamäki, O. Ikkala, R.H.A. Ras, Reliable measurement of the receding contact angle, Langmuir 29 (2013) 3858–3863, https://doi.org/10.1021/la400009m.

[48] A. Work, Y. Lian, A critical review of the measurement of ice adhesion to solid substrates, Prog. Aerosp. Sci. (2018) 1–26, https://doi.org/10.1016/j.paerosci.2018.03.001.

[49] A.J. Meuler, J.D. Smith, K.K. Varanasi, J.M. Mabry, G.H. McKinley, R.E. Cohen, Relationships between water wettability and ice adhesion, ACS Appl. Mater. Interfaces 2 (2010) 3100–3110, https://doi.org/10.1021/am1006035.

[50] Z. Zhang, L. Ma, Y. Liu, H. Hu, An experimental study on the durability of a hydro-/ice-phobic surface coating for aircraft icing mitigation, in: 2018 Atmos. Sp. Environ. Conf., 2018, pp. 1–15.

[51] Y. Liu, Z. Zhang, H. Hu, H. Hu, A. Samanta, Q. Wang, H. Ding, An experimental study to characterize a surface treated with a novel laser surface texturing technique: water repellency and reduced ice adhesion, Surf. Coat. Technol. 374 (2019) 634–644, https://doi.org/10.1016/j.surfcoat.2019.06.046.

[52] N. Saleema, M. Farzaneh, R.W. Paynter, D.K. Sarkar, Prevention of ice accretion on aluminum surfaces by enhancing their hydrophobic properties, J. Adhes. Sci. Technol. 25 (2011) 27–40, https://doi.org/10.1163/016942410X508064.

[53] O. Faix, in: Fourier Transform Infrared Spectroscopy, 1992, pp. 83–109.

[54] A. Lusi, H. Hu, X. Bai, Producing high yield of levoglucosan by pyrolyzing nonthermal plasma-pretreated cellulose, Green Chem. 22 (2020) 2036–2048, https://doi.org/10.1039/d0gc00255k.

[55] D. Jing, A. Lii-Rosales, K.C. Lai, Q. Li, J. Kim, M.C. Tringides, J.W. Evans, P.A. Thiel, Non-equilibrium growth of metal clusters on a layered material: Cu on MoS_2, New J. Phys. 22 (2020), https://doi.org/10.1088/1367-2630/ab84b5.

[56] Y. Liu, C. Kolbakir, H. Hu, X. Meng, H. Hu, An experimental study on the thermal effects of duty-cycled plasma actuation pertinent to aircraft icing mitigation, Int. J. Heat Mass Transf. 136 (2019) 864–876, https://doi.org/10.1016/j.ijheatmasstransfer.2019.03.068.

[57] L. Gao, Y. Liu, H. Hu, An experimental investigation on the dynamic glaze ice accretion process over a wind turbine airfoil surface, Int. J. Heat Mass Transf. 149 (2020) 119120, https://doi.org/10.1016/J.IJHEATMASSTRANSFER.2019.119120.

[58] Y. Liu, L. Ma, W. Wang, A.K. Kota, H. Hu, An experimental study on soft PDMS materials for aircraft icing mitigation, Appl. Surf. Sci. 447 (2018) 599–609, https://doi.org/10.1016/j.apsusc.2018.04.032.

[59] Y. Liu, C. Kolbakir, H.Y. Hu, X.S. Meng, H. Hu, An experimental study on the thermal effects of duty-cycled plasma actuation pertinent to aircraft icing mitigation, Int. J. Heat Mass Transf. 136 (2019) 864–876.

[60] Y. Liu, W. Chen, Y. Peng, H. Hu, An experimental study on the dynamic ice accretion processes on bridge cables with different surface modifications, J. Wind Eng. Ind. Aerodyn. 190 (2019) 218–229, https://doi.org/10.1016/j.jweia.2019.05.007.

[61] Y. Peng, R. Veerakumar, Y. Liu, X. He, H. Hu, An experimental study on dynamic ice accretion and its effects on the aerodynamic characteristics of stay cables with and without helical fillets, J. Wind Eng. Ind. Aerodyn. 205 (2020) 104326, https://doi.org/10.1016/j.jweia.2020.104326.

[62] M. Zou, S. Beckford, R. Wei, C. Ellis, G. Hatton, M.A. Miller, Effects of surface roughness and energy on ice adhesion strength, Appl. Surf. Sci. 257 (2011) 3786–3792, https://doi.org/10.1016/j.apsusc.2010.11.149.

[63] K. Yamauchi, Y. Yao, T. Ochiai, M. Sakai, Y. Kubota, G. Yamauchi, Antibacterial activity of hydrophobic composite materials containing a visible-light-sensitive photocatalyst, J. Nanotechnol. (2011), https://doi.org/10.1155/2011/380979.
[64] E. Herth, R. Zeggari, J.Y. Rauch, F. Remy-Martin, W. Boireau, Investigation of amorphous SiOx layer on gold surface for Surface Plasmon Resonance measurements, Microelectron. Eng. 163 (2016) 43–48, https://doi.org/10.1016/j.mee.2016.04.014.
[65] J. Wang, Y. He, Y. Yang, W. Xie, X. Ling, Research on quantifying the hydrophilicity of leached coals by FTIR spectroscopy, Physicochem. Probl. Miner. Process. 53 (2017) 227–239, https://doi.org/10.5277/ppmp170119.
[66] Y. Liu, H. Hu, An experimental investigation on the unsteady heat transfer process over an ice accreting airfoil surface, Int. J. Heat Mass Transf. 122 (2018) 707–718, http://linkinghub.elsevier.com/retrieve/pii/S0017931017357125. (Accessed 24 February 2018).
[67] K. Zhang, T. Wei, H. Hu, An experimental investigation on the surface water transport process over an airfoil by using a digital image projection technique, Exp. Fluids 56 (2015) 173, https://doi.org/10.1007/s00348-015-2046-z.